DEVELOPMENT OF A THEORETICAL MODEL FOR PREDICTING LOW VELOCITY IMPACT SENSITIVITY OF BUBBLE-SENSITIZED SLURRY EXPLOSIVES

- FINAL REPORT -

BY:

P. KATSABANIS, Ph.D.

SUPERVISOR: DR. A. BAUER

Work on this project was conducted under the auspices of the Canada Centre for Mineral and Energy Technology, Energy, Mines and Resources, Canada.

D.S.S. File Number: 15SQ.23440-4-9027
D.S.S. Contract Serial Number: 0SQ84-00155
CANMET Project Number: 110702
CANMET Scientific Authority: Dr.K.K. Feng

MINING RESOURCE ENGINEERING LIMITED
1555 SYDENHAM ROAD, RR#8
KINGSTON, ONTARIO
K7L 4V4

101 pp

DECEMBER 1987

MICROMEDIA

ABSTRACT

The sensitivity of commercial explosives to low amplitude shock waves was investigated. A calibrated gap test was applied to one standard military explosive, one emulsion and one slurry product. The results of the gap tests were interpreted as acceptor free surface velocity - pressure or acceptor free surface velocity - attenuator thickness curves which can provide thresholds to burning and detonation for the explosives tested. The gap tests were modelled by using the developed hydrodynamic model "GAP" in order to calculate critical energies for the onset of burning. A series of other tests were examined and critical energies for the start of the decomposition of the test explosive were calculated.

TABLE OF CONTENTS

		Page #
LIST OF FIGURES		iv
LIST OF TABLES		v
1.0	LITERATURE REVIEW	1
1.1	Introduction	1
1.2	Numerical Methods	1
1.2.1	The Critical Energy Criterion	1
1.2.2	The Reaction and Growth Model	2
1.2.3	The Forest Fire Model	4
1.2.4	The Bruckman and Guillet Model	7
1.2.5	Discussion on the Theoretical Models	9
1.3	Experimental Methods	10
1.3.1	Discussion on the Experimental Methods	26
2.0	LOW VELOCITY IMPACT ON COMMERCIAL EXPLOSIVES	28
2.1	Introduction	28
2.2	Projectile Tests	28
2.3	Calibrated Gap Tests	29
2.4	Interpretation of the Experimental Results	37
2.5	Results	48
2.5.1	Pressed RDX (ρ = 1.6 g/cc)	50
2.5.2	Slurry A (ρ = 1.15 g/cc)	54
2.5.3	Emulsion A (ρ = 1.15 g/cc)	54
2.6	Discussion	54
3.0	NUMERICAL MODELLING OF THE GAP TEST	64
3.1	Introduction	64
3.2	The Hydrodynamic Calculations	64
3.3	The Pressure Models	69
3.4	The Model for the Donor Charge	70

3.5 The Model for the Attenuator 71
3.6 The Artificial Viscosity 71
3.7 Calculation of Sound Speed 73
3.8 Results 73
3.9 Discussion 81

4.0 CONCLUSION 87

REFERENCES 89

LIST OF FIGURES

FIGURE #		Page
1.	SEQUENCE OF EVENTS LEADING TO A DETONATION (14)	11
2.	TEST ARRANGEMENT SHOWING METHOD OF INITIATING DRIVER EXPLOSIVE (13)	13
3.	RESULTS FOR 15 cm DIAMETER PBX 9404 [13]	15
4.	RESULTS FOR TRITONAL, H-6 AND PBX 9404 [13]	16
5.	SUSAN TEST PROJECTILE	17
6.	THE LOW AMPLITUDE SHOCK INITIATION TEST (LASI) [20].....	24
7.	TYPICAL CURVE SHOWING RELATIONSHIP BETWEEN FREE SURFACE VELOCITY OF THE ACCEPTOR CHARGE AND SHOCK PRESSURE IN THE ATTENUATOR	25
8.	EXPERIMENTAL ARRANGEMENT FOR THE PROJECTILE TESTS	30
9.	PROJECTILE BEFORE IMPACT (A) AND AFTER IMPACT (B) FOR THE CASE OF TARGET FAILING TO DETONATE	32
10.	SLURRY TARGET WHICH FAILED TO DETONATE DUE TO IMPACT	33
11.	PROJECTILES BEFORE IMPACT (A) AND AFTER IMPACT (B) FOR THE CASE OF TARGET DETONATING DUE TO IMPACT	34
12.	EXPERIMENTAL ARRANGEMENT FOR THE CALIBRATED GAP TESTS	36
13.	TYPICAL STREAK CAMERA RECORD FOR THE CASE OF	

DETONATION OF THE ACCEPTOR 38

14. STREAK CAMERA RECORD OF THE CALIBRATED GAP TEST FOR WAXED RDX 39

15. STREAK CAMERA RECORD OF THE CALIBRATED GAP TEST FOR WAXED RDX 40

16. STREAK CAMERA RECORD OF THE CALIBRATED GAP TEST FOR SLURRY A 41

17. STREAK CAMERA RECORD OF THE CALIBRATED GAP TEST FOR EMULSION A 42

18. SHOCK VELOCITY VERSUS PLEXIGLAS THICKNESS FOR THE CALIBRATED GAP TEST 43

19. ATTENUATION OF THE SHOCK WAVE PRODUCED BY THE DONOR IN THE CALIBRATED GAP TEST 45

20. GRAPHICAL METHOD OF OBTAINING SHOCK PRESSURE AND PARTICLE VELOCITY IN UNDER-INITIATED EXPLOSIVE 46

21. PRESSURE-PARTICLE VELOCITY RELATIONSHIPS FOR REACTED AND UNREACTED EXPLOSIVE 49

22. ACCEPTOR FREE SURFACE VELOCITY VERSUS PLEXIGLAS THICKNESS FOR WAXED AND PRESSED RDX 52

23. PRESSURE VERSUS FREE SURFACE VELOCITY FOR WAXED RDX ρ=1.6 g/cc (90% RDX, 10% WAX) 53

24. ACCEPTOR FREE SURFACE VELOCITY VERSUS PLEXIGLAS THICKNESS FOR SLURRY A 56

25. PRESSURE VERSUS FREE SURFACE VELOCITY FOR SLURRY A 57

26. ACCEPTOR FREE SURFACE VELOCITY VERSUS PLEXGLAS

THICKNESS FOR EMULSION A 59

27. PRESSURE VERSUS FREE SURFACE VELOCITY FOR EMULSION A 60

28. STREAK CAMERA RECORD FOR EMULSION A WHERE DELAYED DETONATION OCCURS 62

29. TYPICAL GRID DESCRIBING THE GAP TESTS 65

30. SIMPLIFIED FLOW CHART OF THE "GAP" COMPUTER CODE 67

31. FINITE-DIFFERENCE GRID SHOWING LOCATIONS OF VARIABLES USED IN THE MOMENTUM CONSERVATION RELATIONS 68

32. EXPERIMENTAL AND CALCULATED CURVES SHOWING PLEXIGLAS PRESSURE AS A FUNCTION OF DISTANCE IN THE CALIBRATED GAP TEST 74

33. TYPICAL PRESSURE HISTORIES FOR VARIOUS POINTS ALONG THE AXIS OF THE GAP TEST ARRANGEMENT 75

LIST OF TABLES

TABLE #		Page
1.	PROJECTILE IMPACT TEST RESULTS FOR SLURRY 1, SLURRY 2 AND EMULSION 4	31
2.	EXPERIMENTAL RESULTS FOR WAXED AND PRESSED RDX	51
3.	EXPERIMENTAL RESULTS FOR SLURRY A	55
4.	EXPERIMENTAL RESULTS FOR EMULSION A	58
5.	HOM EQUATION OF STATE PARAMETERS FOR THE DONOR CHARGE	76
6.	HOM EQUATION OF STATE PARAMETERS FOR THE PLEXIGLAS ATENUATOR (10)	77
7.	HOM EQUATION OF STATE PARAMETERS FOR THE UNREACTED SLURRY A	79
8.	HOM EQUATION OF STATE PARAMETERS FOR THE UNREACTED EMULSION A (23)	80
9.	CRITICAL ENERGIES FOR VARIOUS EXPLOSIVE COMPOSITIONS (22, 29)	82

1.0 *LITERATURE REVIEW*

1.1 *Introduction*

Shock sensitivity of explosives has been a popular subject in the literature. However most of the studies on criteria for explosives initiation and modelling of impact sensitivity deal with military high explosives and high velocity impact sensitivity. In the following, the results of the literature survey on the subject of the low velocity impact sensitivity of explosives is presented.

1.2 *Numerical Methods*

Criteria which have been proposed for the initiation of explosives are the following:

1.2.1 *The Critical Energy Criterion*

The critical energy criterion was developed by Walker and Wasley[1]. This criterion states that there is a critical energy per unit area which must be delivered to the explosive in order to obtain initiation. Therefore[1],

$$E = PU_p t \qquad (1.1)$$

where E is the critical energy per unit area

P is the pressure in the explosive due to impact

U_p is the particle velocity of the explosive after impact

and t is the duration of the impulse.

However

$$P = \rho U_p U_s \qquad (1.2)$$

where ρ is the initial density of the explosive and U_s is the shock velocity.

From (1.1) and (1.2)

$$E = P^2 t/(\rho U_s) \qquad (1.3)$$

Assuming that the impedance of the explosive changes only slowly[1] with U_s equation (1.3) can be expressed as

$$E = a P^2 t \qquad (1.4)$$

where a is a constant. This critical energy must be constant in every impact which is just capable of initiating an explosive. An impact with a larger amount of energy should always result in a detonation. The criterion is known as the P^2t criterion[1]. In the case of impacts by projectiles t is the time from the impact until the rarefaction waves from the side of the projectile meet the axis of the projectile.

The P^2 t criterion is a very good engineering criterion which explains the high velocity impact sensitivity of various explosives. However it cannot be applied to every case. For this reason a number of researchers have modified it. According to Walker[2] the criterion is applied ideally to pure chemical explosives.

Hayes[3] suggested that the criterion should be expressed as:

$P^n t$ = constant

where n is a constant (equal to 2 for most high explosives).

Moulard[4] introduced the critical area concept for the initiation of high explosives by impact of small projectiles in conjunction with the critical energy concept.

1.2.2 *The Reaction and Growth Model*

For modelling explosives initiation the Reaction and Growth

model has been one of the major models. Within the frame of a hydrocode, it models the shock initiation of heterogeneous explosives. The Jones - Wilkins - Lee equation of state is used for both the reaction products and the unreacted explosive. The JWL equation has the form[5]:

$$P = A(1-W/R_1V)\exp(-R_1V) + B(1-W/R_2V)\exp(-R_2V) + WE/V \quad (5)$$

where P is the pressure (Mbar)

V is the volume of the material at pressure P divided by the initial volume of the material

E is the internal energy and

A, B, R_1, R_2 and W are adjustable constants.

The constants are normally obtained by performing cylinder tests and hydrodynamic calculations.

The reaction rate is expressed by the equation[5]:

$$\frac{\partial F}{\partial t} = I\ (1 - F)^x n^r + G\ (1 - F)^x F^y P^z \qquad (1.6)$$

with $n = V_0/V_1 - 1$

where F is the fraction of the decomposed explosive

t is the time

V is the specific volume of the shocked unreacted explosive

P is the pressure

I, x, r, G, y and z are constants.

The first term of equation (1.6) is the ignition term and the second the growth term. The origin of the equation can be explained qualitatively. Before the shock wave arrives, the pressure is zero (P=0) and the explosive is unreacted (F=0) so the reaction rate is also zero. When the shock wave arrives, the growth term is zero (because F=0) but the ignition term is non-zero. The ignition term thus yields a finite reaction rate. The

growth term begins to contribute to the decomposition rate as F grows.

According to Lee and Tarver[5] the following equation provides good agreement with the experimental results:

$$\frac{\partial F}{\partial t} = I\ (1 - F)^{2/9}\ n^4 + G\ (1 - F)^{2/9}\ F^{2/3}\ p^z \qquad (1.6)$$

where $z = 1.0 - 2.0$

The above equation has to be calibrated in order to obtain the parameters G and z. This can be done by performing wedge tests.

According to Lee and Tarver the model applies to a wide range of shock initiation stimuli. The model has been used successfully to describe the shock initiation of PBX 9404, PETN and TNT. However in the case of the modelling of the experiments by Green, James, Lee, Chambers and Westmoreland[6], the model resulted only in qualitative results. These experiments involved the low velocity impact of high HMX-content propellants. The calculated threshold velocities for XDT (unknown transition to detonation or delayed detonation), by using the Reaction and Growth model[5] were found to be as much as 25% too high[6]. The reason was suspected to be the increase of the number of the reacting sites upon recompaction of the propellant which was examined. This increase could not be accounted for in the calculations. Obviously the situation would be worse for the case of commercial explosives due to the variety of the nature of the reacting sites (surface of gas bubbles, solid particles etc.).

1.2.3 *The Forest Fire Model*

The Forest Fire model was created at the Los Alamos Scientific Laboratory in order to model the shock initiation of

heterogeneous military explosives and propellants. The Forest Fire model is a semi empirical model based on the experimental Pop plot (relationship between the distance of run to detonation and the pressure) the reactive and non reactive Hugoniots, the HOM equation of state and the single curve build-up hypothesis. The technique has been applied to commercial explosives by the author under a contract from CANMET, awarded to Mining Resource Engineering Limited. It was proven that the Forest Fire model is suitable for the modelling of the shock sensitivity of slurries and emulsions[7,23]. However the technique, since it is a shock sensitivity model examining the shock initiation of heterogeneous explosives is not suitable to describe the ignition of slurries and emulsions due to low velocity impacts.

An attempt has been made by Forest and Mader[8,9,10] to model the burning to detonation transition for propellants. The modelling was done in order to simulate accidents occurring in rockets containing damaged propellants. A brief summary of this effort is discussed in the following[8,9,10,11].

A part of the propellant is assumed to be burning. The burning of the material can produce a shock, which, if it is strong enough, will initiate the explosive. Therefore a model for the burning and a model for the shock to detonation transition are required. The bulk burning is used to simulate the burning of a porous bed of propellant that is assumed to be ignited over all burning surface simultaneously. The explosive is assumed to be divided into uniform pieces of similar geometry which burn at a linear burn rate perpendicular to the surface of each particle.

The porous explosive is burnt according to the surface regression rate[8],

$$X' = C\,P^{n}$$

where C and n are constants and

P is the pressure.

The mass burn rate is,

$$\frac{dM}{dt} = - S \rho X' \qquad \text{or}$$

$$\frac{dM}{dt} = -\left(\frac{S_0}{V_0}\right)\left(\frac{S}{S_0}\right)(\rho_0 V_0)\left(\frac{\rho}{\rho_0}\right)X' \qquad (1.7)$$

where S and V refer to surface area and volume of the explosive respectivelyand the subscript 0 refers to the initial state.

The fraction of undecomposed explosive is:

$$W = \frac{M}{M_0} = \frac{M}{\rho_0 V_0} \qquad (1.8)$$

Therefore from equation (1.7),

$$\frac{dW}{dt} = -\left(\frac{S_0}{V_0}\right)\left(\frac{S}{S_0}\right)\left(\frac{\rho}{\rho_0}\right)X' \qquad (1.9)$$

However the ratio ρ/ρ_0 is close to 1 for the pressures of burning[8]. Therefore,

$$\frac{dW}{dt} = -\left(\frac{S_0}{V_0}\right)\left(\frac{S}{S_0}\right)X' \qquad (1.10)$$

The ratio S_0/V_0 can be found from the density and the porosity of the explosive while the ratio S/S_0 depends on the shape of the burning particle. For example for spherical particles

$$\frac{S}{S_0} = W^{2/3}$$

Ignition in the model is simply the onset of burning. There is no account for the ignition process and the ignition is taken to be complete throughout the porous bed region. Therefore the model can describe the behaviour of the explosive once violent burning has commenced. The violent burning can result in a shock somewhere in the system, especially under conditions of confinement.

The initiation due to the shock is modelled by the

Forest Fire technique. As soon as some specific value of pressure pulse is generated the Forest Fire model is turned on. If the pressure pulse is sufficient, detonation will occur; if not the result is a failure.

In this model one has to assume that the porous bed is ignited by some mechanism. As such this model is not suitable for the low velocity impact initiation of slurries and emulsions since no mechanism is provided for the onset of burning. Furthermore the porous bed of damaged explosive is difficult to be described quantitatively. For these reasons the method has been used to improve the understanding of accidents rather than to predict the critical conditions which can lead to an accident.

1.2.4 *The Bruckman and Guillet Model*

Bruckman and Guillet[12] calculated the critical temperature inside a hot spot, required to initiate an explosive, by solving the heat balance equations for the thermal decomposition and considering the effect of depletion of the reagent. Their calculations, although able to describe the effect of the hot spot geometry and the Arrhenius parameters on the critical temperature, cannot be applied to commercial explosives. Commercial explosives are highly heterogeneous containing bubbles of various sizes and various shell types as well as solid particles of a variety of materials (Aluminum, inorganic salts etc.) and sizes. It is obvious that these variables cannot be modelled in a precise method, since they are not known or cannot be found exactly.

Furthermore the model is a thermal initiation model which predicts initiation or failure given the initial temperature. In order for this to be applicable to impact conditions, the exact

nature of the hot spot has to be known. According to Bowden and Yoffee[33], there are three factors creating hot spots in heterogeneous explosives. These are:

a. Voids within the explosive.

b. Regions where the explosive is heated by viscous flow or plastic deformation, when rapidly flowing explosive escapes between impacting surfaces.

c. Points of friction at the surface of the container walls, or grit particles or crystals of explosive.

All three categories can be present in an impact experiment and obviously the relative importance of each has to be quantified. It is worth mentioning that there is considerable disagreement between scientists with regard to the mechanism by which hot spots are created. For example, it has beem proposed that gas bubbles in the mass of the explosive heat adiabatically and decomposition starts. This theory has been unsatisfactory in explaining how heat transfer can take place at a fast enough rate for detonation to occur[31]. For this reason other theories have been proposed.

Ljundberg has found[31] that jetting due to the assymmetric collapse of the voids in the explosive can be a reason for detonative behaviour of an impacted explosive. Furthermore Mader[10] proposed the hydrodynamic hot spot. According to him the shock wave interacts with density discontinuities (voids, particles etc.) and the resulting convergence of shocks creates spots of high pressure and temperature. These spots decompose, liberating energy which strengthens the shock until finally detonation occurs.

Mader[10] modelled the creation of the hot spot by using two

dimensional hydrodynamics to study theoretically the formation of hot spots interacting with spherical, cylindrical or biconical voids and with cylinders and spheres of aluminum. However this modelling covered only cases where some well known inhomogeneities had been introduced in a homogeneous mass. Recently three dimensional modelling was performed by Mader[34] by using supercomputers and the 3DE code. In these models the effectiveness of the hydrodynamic hot spot was demonstrated. However the size of the explosive which was modelled was very small (a cube having sides with length of 0.2 cm). Obviously, such modelling is not possible in an actual situation where a variety of density discontinuities will appear distributed randomly inside the explosive mass with a spatial distribution much larger than the one which can be modelled by the three dimensional models. Therefore a completely theoretical approach of modelling the hot spot is not feasible at the present time.

1.2.5 *Discussion on the theoretical models*

The Forest Fire model and the Reaction and Growth model have been developed to model the shock to detonation transition of explosives. Both of them are semiempirical requiring difficult experiments in order to predict shock sensitivity. The Reaction and Growth model has been used to predict low velocity impact sensitivity with limited success. The Forest Fire code has been modified to model the burning to detonation transition of damaged explosives. The model cannot be used to predict low velocity impact sensitivity unless the transition from impact to burning can be modelled and the thickness of the burning explosive can be found.

A complete theoretical approach requires the modelling of the hot spot. This would require the knowledge of the mechanism of the hot spot and the geometrical position of every density discontinuity in the explosive. The exact mechanism of a hot spot is not exactly known and a representative sample would have dimensions necessitating computing power beyond the capability of todays computers. Therefore a semiempirical approach is preferable.

1.3 *EXPERIMENTAL METHODS*

Most of the experimental results regarding projectile impact sensitivity incorporate velocities of more than 500m/s. Results for low velocity impact sensitivity are limited.

However it has been recognized[11] that impacts in the low velocity regime, although unable to detonate the explosive due to the shock to detonation transition, are able to start a reaction in the explosive which can lead to a detonation.

Smith and Craig[14] have presented a series of events which can lead to an accidental detonation. This is shown in Figure 1[14]. An accident can enter the chain at any point. Normally the accident starts with breakup and ignition which can start simultaneously or in either order[14]. The process can lead to a deflagration and the deflagration can result in a shock wave somewhere in the system. The shock wave, if it is strong enough will shock initiate the explosive and detonation will occur. Therefore a very important concern in safety considerations is the critical impact energy which will ignite the explosive. In many cases the ignition leads to a deflagration which is violent enough so that it is considered a catastrophic event.

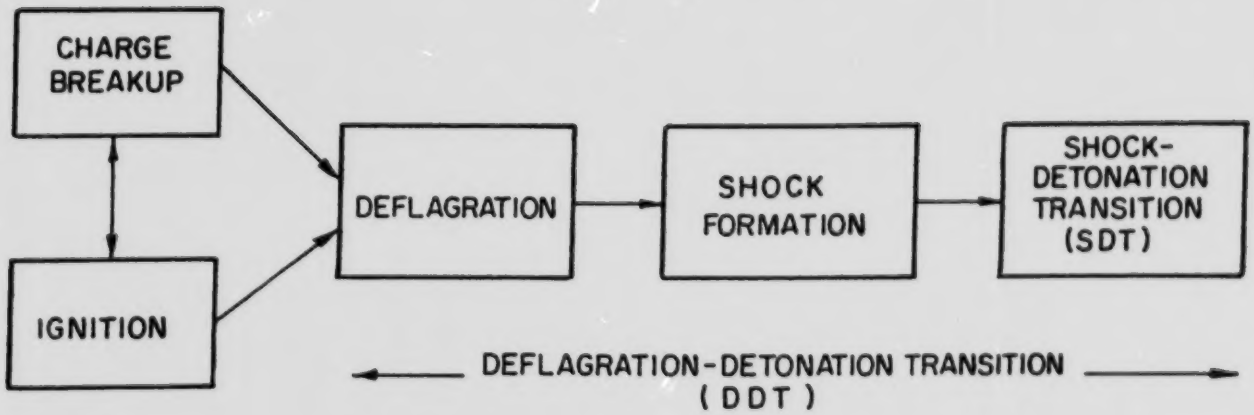

FIGURE 1: SEQUENCE OF EVENTS LEADING TO A DETONATION [14].

It is worth noting that the understanding of the phenomena involved declines rapidly as we move from right to left on the above sequence. The phenomena of the shock to detonation transition have been investigated both experimentally and theoretically with sufficient detail. The deflagration of an explosive is known less and the ignition mechanism is the least known. Furthermore the event may stop at any point in the sequence without leading to a detonation. In many experiments (e.g. projectile impact) this is considered to be a failure. However the result may be such that under a small change of conditions detonation or a violent deflagration can occur. This will depend on many parameters such as confinement, porosity, extent of damage to name a few. For this reason experimental results normally do not indicate the probability of a charge to detonate when it is given a certain amount of energy. In the following experimental results and methods investigating the behaviour of explosives due to low velocity impacts will be discussed.

Napadensky[13] has reported initiation of PBX 9404 at an impact velocity of 134m/s (440ft/s). The experimental set up is shown in Figure 2. The fragmentation of the Aluminum disk results in an impact of the low density explosive at various points simultaneously. Thus the low density explosive detonates and drives the steel plate which impacts the test explosive. By varying the quantity and the density of the low density explosive plate velocities between 70 and 610 m/s were achieved. This experiment was designed to simulate the loading conditions which are imposed during an accidental impact[13].

The interesting finding of Napadensky's work is that the

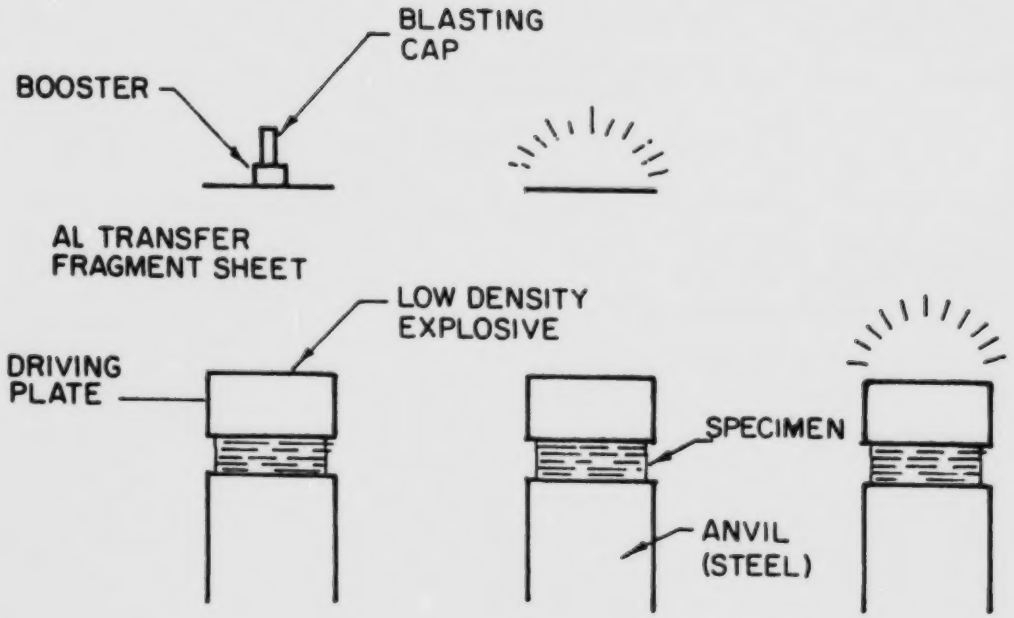

FIGURE 2: TEST ARRANGEMENT SHOWING METHOD OF INITIATING DRIVER EXPLOSIVE [13].

initiation of the explosive when impacted by a plate depends on the length of the explosive target. Her results are summarized in Figures 3 and 4. For a fixed diameter the required minimum impact velocity to initiate the charge increases with the length of the specimen. However when shock to detonation results at the first passage of the impacting shock wave, any increase in length does not change the behaviour of the target.

At lower velocities detonation is delayed and results after significant crushing of the specimen or after crushing and pinching.

In region A (Figure 3) the detonation occurs during the first passage of the shock wave (shock to detonation transition). In region B the detonation occurs 100μsec to 1msec after impact and in region C 1-3 msec after impact. Obviously the B and C regions are of interest for the low velocity impact sensitivity. It appears that detonative behaviour is associated with a significant amount of damage in the test sample.

The Susan test has been used extensively by military laboratories to investigate the relative sensitivity of an explosive under "field conditions" of impact. The Susan projectile is shown in Figure 5. The explosive test sample weighting 0.4Kg is loaded in the Susan projectile and fired against a steel target. The overpressure from the impact induced reaction is recorded by using pressure gauges placed at various distances. The result is expressed as TNT equivalent weight to produce the same overpressures if detonated in the geometry of the Susan test. A large number of results of Susan tests has been published by the Lawrence Livermore Laboratory[29]. It has been obrerved that some explosives like Composition B and PBX 9011 have

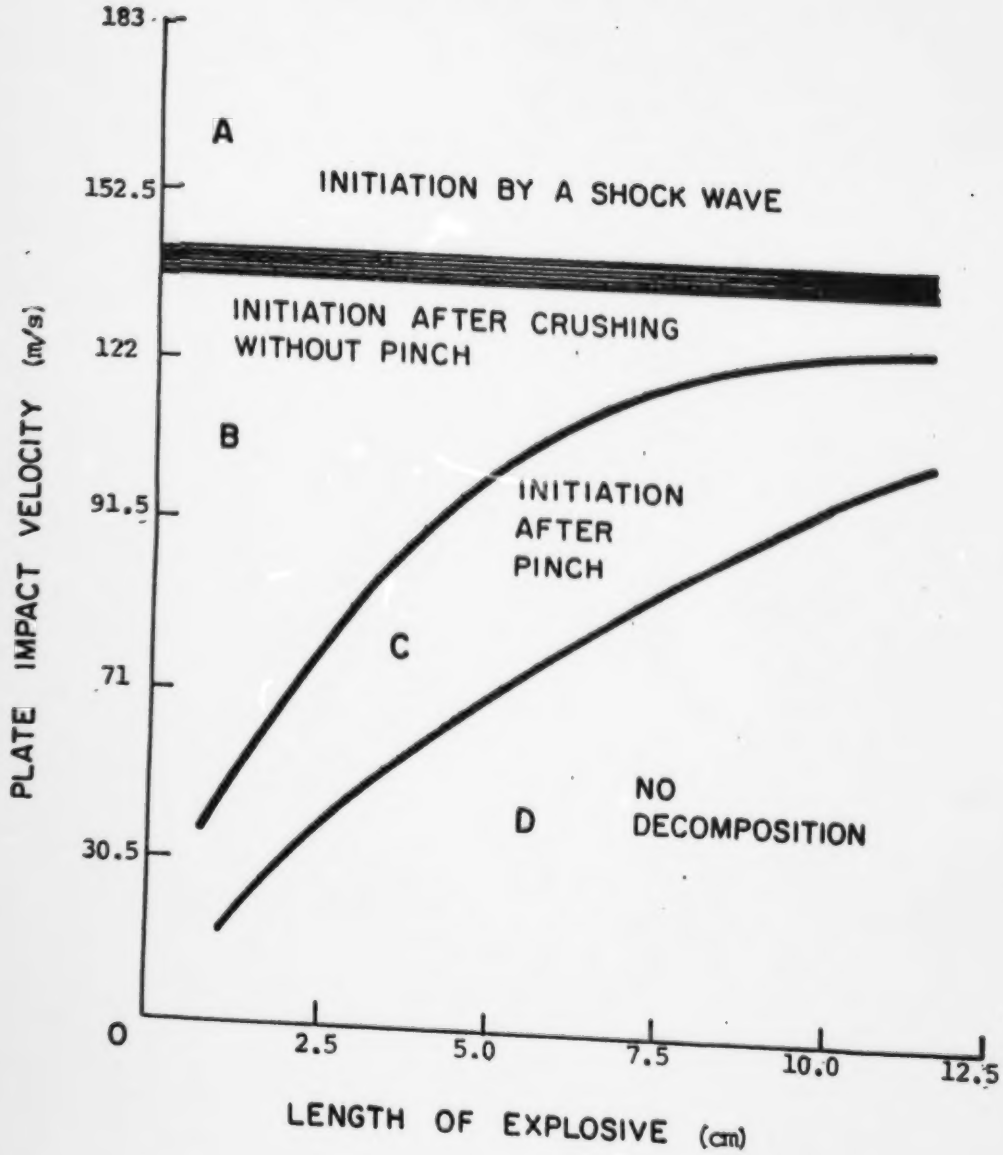

FIGURE 3: RESULTS FOR 15 cm DIAMETER PBX 9404 [13].

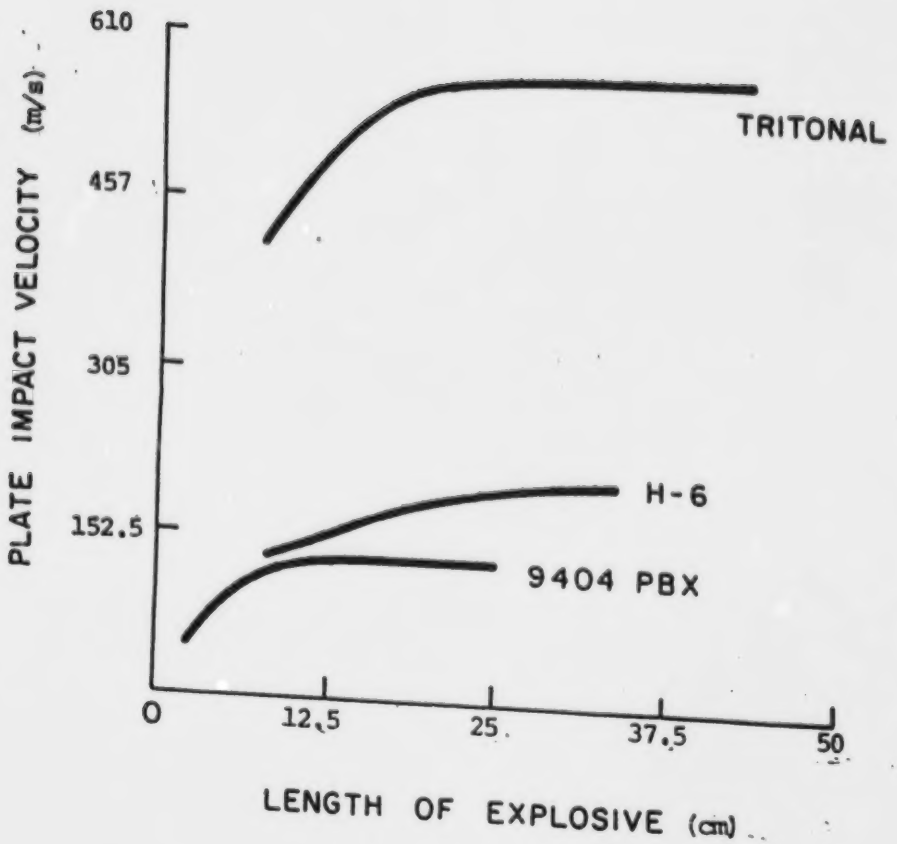

FIGURE 4: RESULTS FOR TRITONAL, H-6 AND PBX 9404 [13]

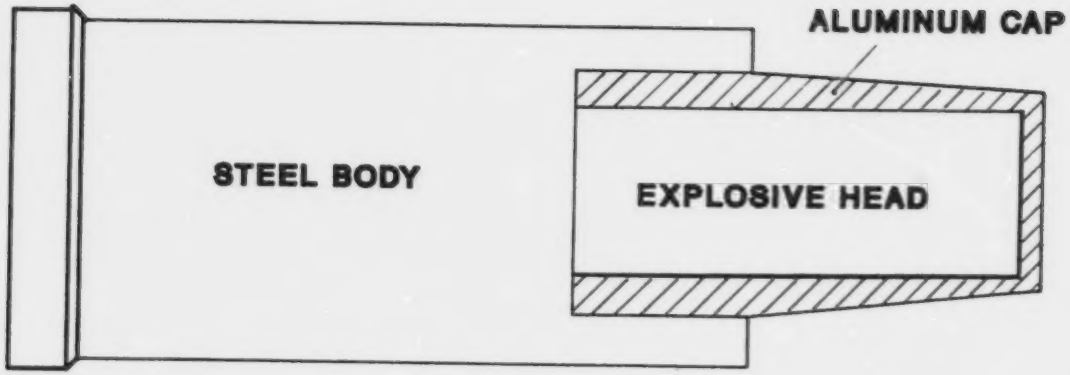

FIGURE 5: SUSAN TEST PROJECTILE

ignition thresholds at about 50 m/s with reaction enhancement only at the pinch stage of the impact. Others like LX-09-0 and LX-10-0 have ignition thresholds of about 30 m/s and high reaction levels early at the impact stage (before pinching). These reactions build to violent levels rapidly indicating compositions susceptible to low velocity impacts.

Green and Dorough[15] investigated the ignition and the detonative behaviour of explosives subjected to low velocity impacts experimentally by performing Susan tests and anvil-driver tests. These tests were selected to test the explosives under conditions of crushing impact. A summary of these tests is provided in the following:

The Susan test has already been described previously. In the rest of the tests, explosives were attached to driver plates which were thrown against steel targets. The steel driver plate had a diameter of 20.3 cm and a thickness of 2.54 cm. In type 1 test the explosive had a diameter of 5.1 cm and a length of 10.2 cm. In type 2 test the explosive was 2.54 cm thick and the diameter was 10.2 cm.

Type 1 test results in fracturing of the solid explosive due to impact. The initial compression is relieved by this mechanism. However, some time later the broken explosive is trapped and recompacted between the driver plate and the target plate. Ignition happens when the explosive is in a divided state.

In type 2 experiments the disk of explosive is under compression during the entire course of impact. The explosive is forced to flow out at high rates. Ignition is due to pinching of the explosive between the plates.

Test 1 produced the following results[15]:

For the explosive LX-04-01 (HMX 85%, Viton 15%, ρ=1.86 g/cc) detonations were observed at velocities above 54 m/s while burning started at about 40 m/s. Composition B (ρ=1.715g/cc) detonated at velocities as low as 78 m/s. Ignition however started at 69 m/s. It is worth mentioning that detonations did not always happen at velocities above 78 m/s. Occasionally deflagrations would be observed.

For PBX-9011 (HMX 90%, Estane 10%, ρ=1.77 g/cc) ignition started at 80 m/s. Detonation was not reported.

PBX-9404 (HMX 94%, NC 3%, CEF 3%, ρ=1.84 g/cc) exhibited the same erratic behaviour as Composition B. Detonation was observed at 47.5 m/s without any noticeable reaction at lower velocities. At velocities higher than 47.5 m/s both deflagrations and detonations were observed.

Test 2 produced the following results:

LX-04-01 detonated at an impact velocity of 50 m/s while at higher velocities both deflagrations and detonations were reported.

Composition B started burning at 62 m/s, detonated at 70 m/s but produced both deflagrations and detonations at velocities higher than 70 m/s.

PBX 9011 started burning at 58 m/s. No detonations were observed.

Finally PBX-9404 deflagrated violently at impact velocities above 39 m/s. It is obvious that detonations are rather unpredictable in these tests.However if the ignition of reaction is recorded, the obtained results by the various geometries of impact do make sense.

Hay and Watson[16] have reported threshold projectile

velocities in the range between 24 and 90m/sec impacting air bubble sensitized Nitromethane, aqueous solutions of amine nitrate, Dinitrotoluene and n-Propylnitrate. The low velocities were obtained by a sudden release of pressurized air through a gun. The targets were confined in steel cylinders having an internal diameter of 10.2cm and a length of 15.2cm. The projectile (steel) had the following dimensions;

diameter : 9.84cm

length :13.30cm

weight : 8.10kg

The results were reported as positive if reaction occurred. Therefore the threshold velocities which were reported correspond to threshold velocities for ignition. The surprisingly low threshold velocities might be due to the strong confinement of the target explosives. Confinement can result in shock reverberations inside the target and to substantial pressure buildup.

Frey, Melani, Chawla and Trimble[17] have investigated the role of confinement on projectile impact. According to them, an unconfined explosive or an explosive confined at the front (impacted) face exhibits a shock to detonation transition if the shock created by the impact is sufficiently strong. On the contrary, when a projectile impacts a charge which is fully confined, violent reactions at low velocity impacts can be observed. These reactions can result in a delayed detonation. In their work steel cubic projectiles were used, which hit confined targets of Composition B, Octol and PBX 9404. It was found that there was a transition from essentially no reaction to a violent explosion over a very narrow range of velocities. The transition from no reaction to violent explosion occurred in all cases at a velocity change of less than 200m/s. The researchers concluded

that confinement was essential in achieving low velocity impact generated explosions[17]. However it was also noticed that in some cases the confinement ought to be sufficiently strong (especially for Composition B). The reason for the behaviour of confined charges was attributed to shock reverberations caused by the confining material[17].

Experimental studies performed by Green, James, Lee Chambers, Tarver, Westmoreland, Weston and Brown[6] showed that high HMX-content(40-50%) propellants can undergo delayed detonation when they are subjected to axisymmetric impacts, although the pressure is less than the one required for shock to detonation transition. The time from ignition to detonation was found to be between 10 and 30μsec. The time from impact to detonation was reported to be between 100 and 400μsec and the threshold projectile velocities were between 150 - 180m/sec. The projectile had a 155mm diameter and its weight was 24.5kg. The low velocity impact detonations were attributed to the rarefaction/recompaction of the propellant due to the impact. Low velocity impact detonations under single impact have been observed under special conditions (normal impact, flat surfaces, aspect ratio greater than 0.6).

Hercules Incorporated[19] developed an instrumented shotgun facility to investigate impact-related phenomena in solid rocket propellants. Two types of tests were conducted; direct impact and pickup.

In the direct test an 8gm propellant projectile (17mm diameter, 20mm length) is thrown against a steel plate. Three types of decomposition reactions were identified:

Deflagration

Shock to Detonation transition (SDT)

Delayed detonation (XDT)

SDT occurs during the first passage of the shock wave generated by the impact, through the propellant cylinder. The time from impact to detonation is normally less than 5μsec.

Delayed detonation (XDT) occurs after the propellant cylinder is severely deformed and damaged. The time from impact to detonation is normally larger than 30μsec.

It was found in these tests that shock to detonation transition occurred at projectile velocities of more than 762m/sec (2500ft/sec) while deflagrations occurred at velocities less than that. Delayed detonations occurred at velocities between 366 and 762m/sec. It was found that about 25% of the impacts in the above regime resulted in delayed detonations while the rest of the impacts resulted in deflagrations. It is obvious that deflagrations and delayed detonations occurred under practically identical conditions.

In the pickup tests a propellant projectile impacts a propellant disk and the composite mass of the damaged propellant impacts a target plate. It was found that the probability of having a delayed detonation (XDT) increased by this type of experimental arrangement. Therefore delayed detonations occur in the case of propellants which are highly damaged and fragmented. Obviously it is very difficult to differentiate between the critical conditions for deflagration and for delayed detonation. It seems to us that the determination of a threshold to ignition or decomposition should be the critical point as far as safety is concerned.

Tasker[20] has performed work along these lines. He has

designed a modified gap test which allows the measurement of the critical pressure for reaction of the tested acceptor charge. The experimental arrangement for the so called Low Amplitude Shock Initiation (LASI) test is shown in Figure 6. The donor is made of tetryl with dimensions of 51mm in diameter and 51mm length. The acceptor charge has a diameter of 51mm and thickness of 12.7mm. The attenuator is made of plexiglas of varying thickness. The top surface of the acceptor is photographed by a high speed framing camera. The velocity of the free surfaces of the acceptor charge is obtained from the frames. By calibrating the plexiglas gap it is possible to establish the relationship between the pressure in the plexiglas and the initial free surface velocity of the acceptor plate. A typical result is shown in Figure 7[20]. In the low pressure region the explosive does not react. As the pressure is increased decomposition starts and the free surface is accelerated. If the pressure is high enough detonation occurs. The surface velocity is constant above the detonation threshold.

This arrangement has been used on a variety of military explosives and propellants.

A very similar test arrangement has been used by Liddiard and Forbes of the Naval Surface Weapons Center[21] to test the low impact pressure sensitivity of cast H-6 and PBXW-109. The only difference between this test and the previous one is the donor charge which in this case is made of pentolite. It was found that the threshold pressures for H-6 and PBXW-109 were 17.5 and 18Kbar respectively. It is worth mentioning that the pressure thresholds for detonation are 58 and 74Kbar respectively[21].

Recently (1985), Kroh, Thoma, Arnold and Wollenweber[22] tried the same arrangement in order to obtain threshold low impact

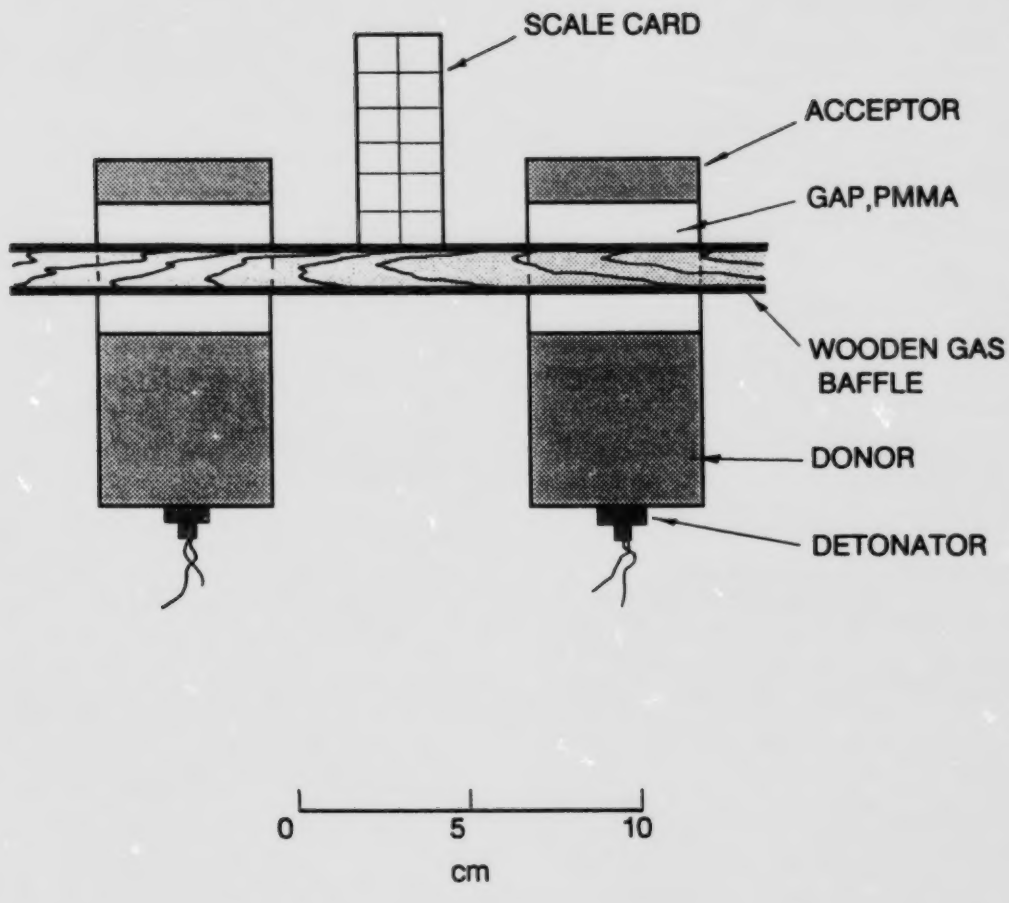

FIGURE 6: THE LOW AMPLITUDE SHOCK INITIATION TEST LASI [20].

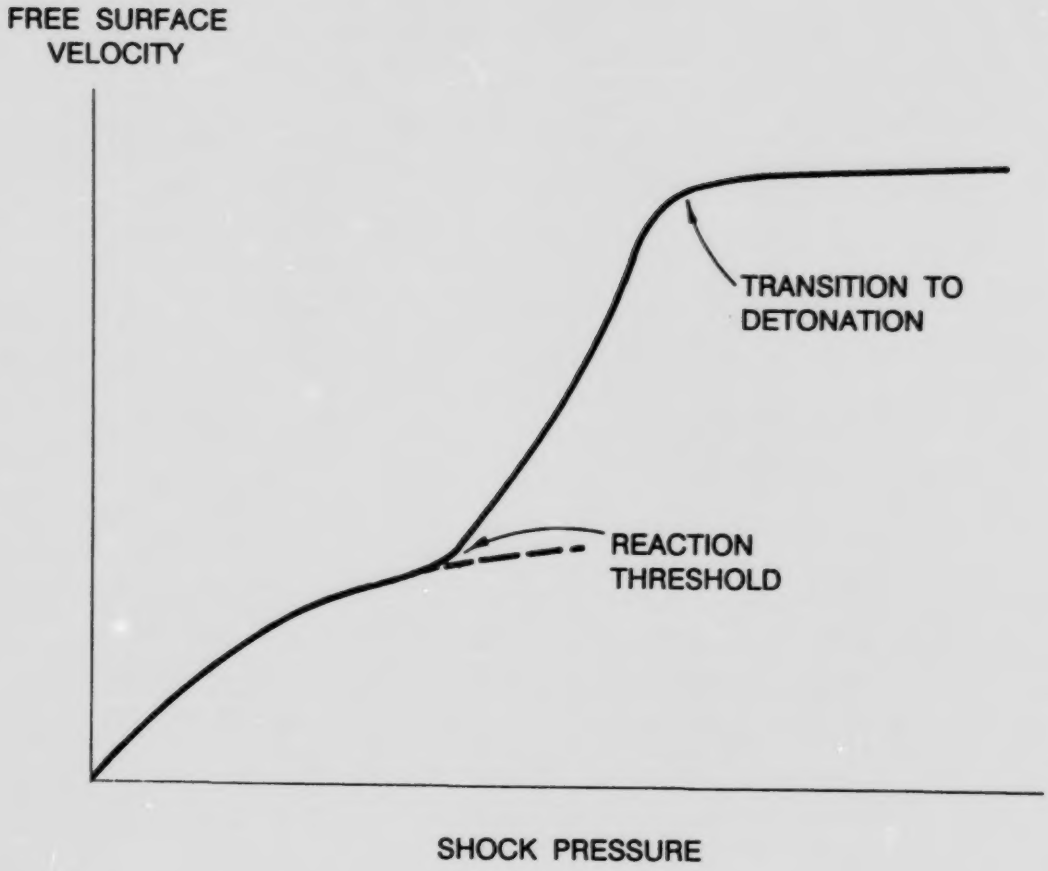

FIGURE 7: TYPICAL CURVE SHOWING RELATIONSHIP BETWEEN FREE SURFACE VELOCITY OF THE ACCEPTOR CHARGE AND SHOCK PRESSURE IN THE ATTENUATOR

pressures for the start of decomposition of explosive targets. The explosives tested were HNS (ρ =1.60g/cc), TNT (ρ =1.60g/cc), HMX/PB (85/15) (ρ =1.71), RDX/AL/PB (67/18/15) (ρ =1.55g/cc and 1.65g/cc) and RDX/AL/PB (71/14/15) (ρ =1.65g/cc). The donor charge consisted of Tetryl with a diameter of 57.5mm and length of 50mm and the acceptor charge had a diameter of 57.5mm and length of 20mm. The results were reported as pressure-escape velocity curves. The German investigators recognized that the threshold pressures obtained by the test are dependant not only on the composition and the physical state of the acceptor material but on the experimental arrangement as well. The dimensions influence the result since they control the times at which rear and lateral rarefaction waves arrive at the shock front. The explosive response is dependant on the duration of the shock pulse and on the peak pressure of the pulse. Therefore the values obtained are valid only for the specific test arrangement employed by the laboratory which conducted the test. It was suggested[22] that the pressure time profile be specified in each test. If the pressure profile is known then the integral $\int P\, U_p dt$ can be calculated. This value provides the critical energy for the start of decomposition and it is not test dependant. For the calculations a computer code based on Lagrangian dynamics was used. The detonation of the donor was modelled by using the C-J burn technique with the JWL equation of state.

1.3.1 *Discussion on the Experimental Methods*

From the above it follows that the behaviour of an explosive subjected to impact can be detonative or not depending on the test configuration, duration of impact, deformation of the sample and confinement. It seems that the final result is not always the

same although the initial conditions are similar. In the low velocity range, impacts generate only very low amplitude stress waves which are too weak to shock initiate the explosive. The primary mechanicm in this case is some form of frictional heating or concentration of the impact energy to limited regions of the explosive which decompose producing a deflagration which continuous, dies out or builds to a detonation depending on the explosive and the impact geometry. Furthermore the physical state of the explosive during impact changes, complicating the phenomenon since it creates additional reaction centres and changes the density. Delayed detonation cannot be a criterion for the behaviour of an explosive due to low velocity impact.

However the ignition of the explosive is more interesting since it provides a necessary (but not sufficient) condition for detonation to occur. Therefore it is worth trying to examine the conditions leading to ignition and correlate ignition to critical impact energy for the various impact experiments.

2.0 *LOW VELOCITY IMPACT ON COMMERCIAL EXPLOSIVES*

2.1 *Introduction*

The sensitivity of commercial explosives to low velocity impacts is very important since the major concern of the users and the manufacturers is safety under normal application. Low velocity impacts are of concern because they are common in ordinary accidents (traffic etc.) and as it has been clear in the previous chapter they are a recognized source of accidents in the area of military explosives. Low velocity impacts or low amplitude shock waves can be a cause of a violent event which can lead to a major catastrophy. For this purpose the sensitivity of commercial products to low velocity impacts was examined experimentally and theoretically. Initially large diameter projectile tests were performed in order to investigate if low velocity impacts would lead to detonation. Later the effort was concentrated in establishing the low amplitude impact sensitivity of commerical explosives by using well calibrated gap tests. The tests were modelled numerically and the critical energy for ignition was calculated.

2.2 *Projectile tests*

In order to determine the susceptibility of slurry explosives to low velocity impacts, aluminum projectiles were fired from a cannon towards targets of slurry explosives. A series of tests was conducted by varying projectile velocity and diameter. The projectile diameters used were 2.5cm, 5.1cm, 10.2cm

and 15.4cm. The slurry targets were tested unconfined and confined in steel tubes. The projectile velocity was calculated by reading the time interval for passage of the projectile between two light sensors placed a known distance apart in front of the explosive target. The impact was observed by a high speed camera having a writing speed of 3000 frames per second. Thus the detonation or failure of the target was determined . The experimental set up is shown in Figure 8. The results of the firings are shown in Table 1.

After each test the projectile is recovered. Figure 9 shows a projectile before and after the impact in the case of a charge failing to detonate. Figure 10 shows the slurry target. Figure 11 shows projectiles before and after impact for the case of a detonation.

From the results of Table 1 it follows that the slurries tested did not detonate from low velocity impacts. Confinement seems to have a significant effect on the susceptibility of the explosives to impact initiation. Modelling of the above results proved that the detonations were due to the shock provided by the impact. Therefore the case was a case of Shock to Detonation Transition (SDT).

2.3 *Calibrated Gap Tests*

After conducting the projectile tests, it was obvious that the main concern is not the transition to detonation due to a low velocity impact but rather the ignition of a reaction which may or may not result in a detonation. For this purpose a calibrated gap test was used. The test is similar to the one implemented by Tasker[20], NSWC[21] and Kroh[22]. The

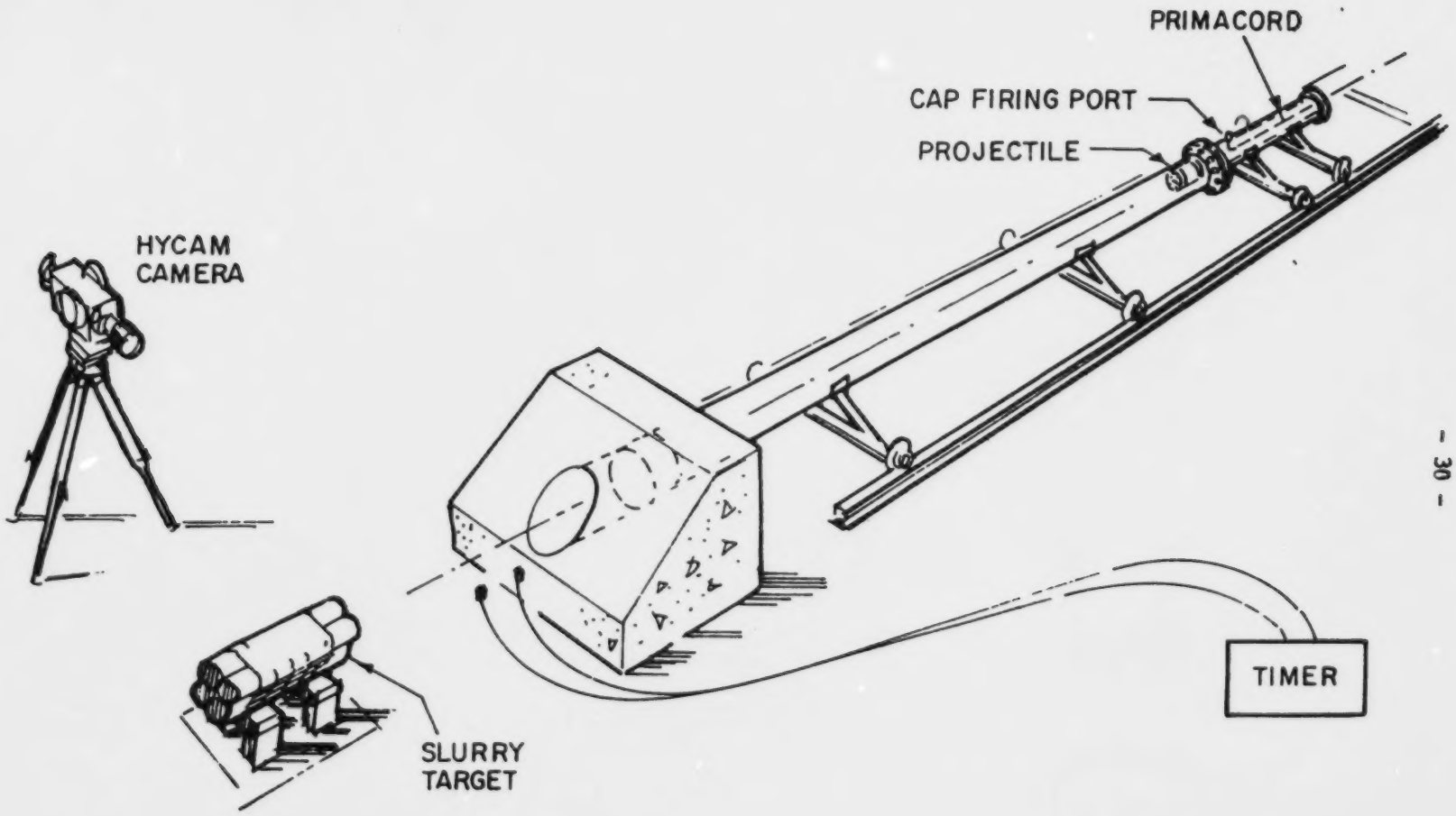

FIGURE 8: EXPERIMENTAL ARRANGEMENT FOR THE PROJECTILE TESTS.

TABLE 1: PROJECTILE IMPACT TESTS FOR SLURRY A SLURRY B AND EMULSION A

MEASURED PROJECTILE VELOCITY (m/s)	SLURRY A					SLURRY B			EMULSION A
	PROJECTILE DIAMETER (mm)								
	25[3]	25[1]	50[4]	100[5]	152[6]	25[3]	50[4]	152[6]	25[3]
33	-	-	F[2]	-	-	-	-	-	-
34	-	-	F	-	-	-	-	-	-
39	F	-	-	-	-	-	-	-	-
46	-	-	F	-	-	-	-	-	-
67	-	-	F	-	-	-	-	-	-
70	F	-	F	-	-	-	-	-	-
132	-	-	-	-	F	-	-	-	-
135	-	-	-	-	-	-	-	-	-
141	-	-	F	-	-	-	-	-	-
162	-	-	-	-	-	-	-	F	-
190	-	-	-	-	F	-	F	-	-
219	-	-	F	-	-	-	-	-	-
228	-	-	-	-	-	-	-	-	-
264	-	-	-	F	-	-	-	-	-
277	-	F	-	-	-	-	-	-	-
286	-	F	-	-	-	-	-	-	-
296	F	-	-	-	-	-	-	-	-
316	-	-	-	-	-	-	-	-	-
330	-	-	-	F	-	-	-	F	-
337	-	D	-	F	-	-	-	-	-
342	-	-	-	-	-	-	F	F	-
344	-	-	F	F	D	-	-	F	-
347	F	-	D/F	-	-	-	-	-	-
350	-	-	D	D	-	-	-	-	-
356	-	D	-	-	-	-	F	-	-
358	-	-	-	-	-	-	-	-	-
368	-	D	-	-	D	-	-	F	-
369	-	-	-	-	-	-	-	-	-
380	-	-	-	-	-	-	-	D	-
396	-	-	-	-	-	-	-	F	F
410	-	D	-	-	-	-	D	-	-
417	-	-	-	-	-	-	-	-	-
421	-	D	-	-	-	-	-	-	F
444	D	-	-	-	-	-	-	-	-
460	-	-	-	-	-	F	-	-	-
537	D	-	-	-	-	D	-	-	F
						-	-	-	F

1. Confined in steel pipe (schedule 40 with i.d. of 50 mm
2. F = Failure D = Detonation
3. Projectile length 50 mm
4. Projectile length 100 mm
5. Projectile length 180 mm
6. Projectile length 152 mm

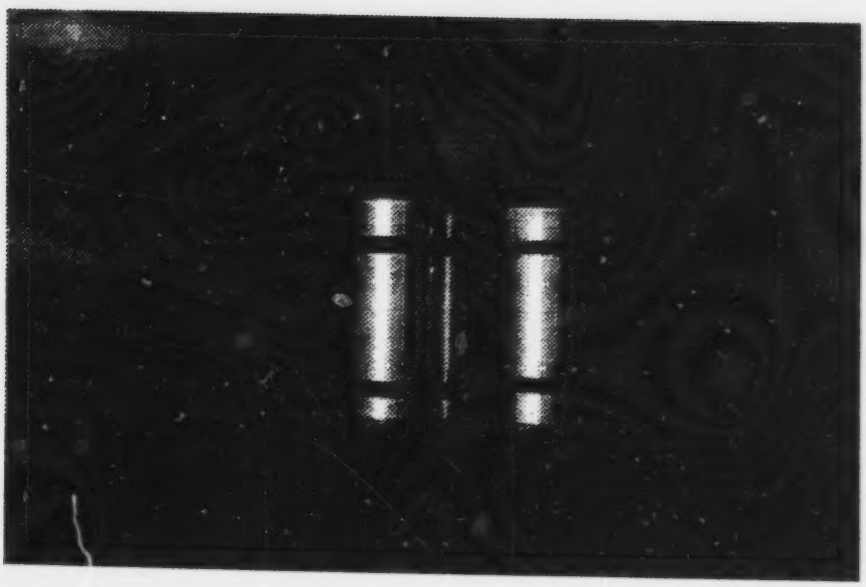

FIGURE 9: PROJECTILE BEFORE IMPACT (A) AND AFTER IMPACT (B) FOR THE CASE OF TARGET FAILING TO DETONATE.

FIGURE 10: SLURRY TARGET WHICH FAILED TO DETONATE DUE TO IMPACT

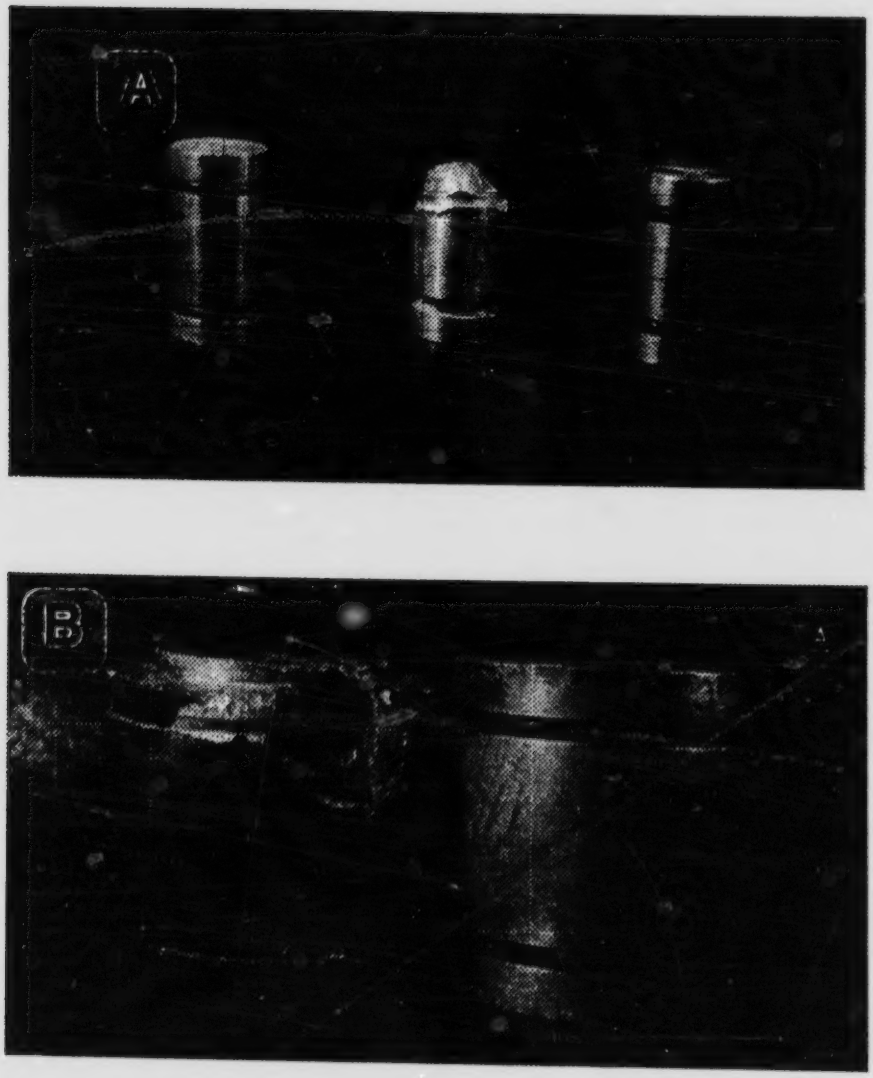

FIGURE 11: PROJECTILES BEFORE IMPACT (A) AND AFTER IMPACT (B) FOR THE CASE OF TARGET DETONATING DUE TO IMPACT.

experimental set up is shown in Figure 12. The test consisted of a donor charge, an attenuator plate an acceptor charge and an argon filled light bomb. The free surface velocity of the acceptor plate is recorded as a function of the thickness of the plexiglas attenuator. The donor is made of three disks of pressed RDX (90% RDX, 10% wax). Each disk has a diameter of 7.64cm and a height of 2.54cm. The density of the charge is 1.55g/cc The attenuator is made of square plates of plexiglas with dimensions of 17.8cm x 17.8cm. The block of plexiglas is normally polished so that it is transparent. The acceptor has the same diameter as the donor and a height of 2.54cm and it is placed in such a way that they have a common axis of symmetry. The various parts of the test (donor, attenuator, acceptor) are glued carefully with plexiglas glue so that no air-bubbles are included in the mass of the donor, acceptor and attenuator orat the interfaces. When emulsions and slurries were used as acceptor charges, they were placed directly on the plexiglas attenuator. Care was taken not to include any air bubbles at the interface. Furthermore the charge is placed in such a way that the free face of the acceptor is exactly perpendicular to the slit of the streak camera.

The donor is initiated by a 10g PETN primer and the event is recorded by using a streak camera. The slit of the camera is placed at the centre of the charge, parallel to the axis of symmetry of the charge. At a specific time the light bomb is detonated to produce the back light necessary for the shadow graphic streak camera technique. From the cutoff of this light, as the shock wave passes through the plexiglas, it is possible to obtain the shock velocity in the plexiglas attenuator as a function of thickness of the plate. Furthermore when the shock

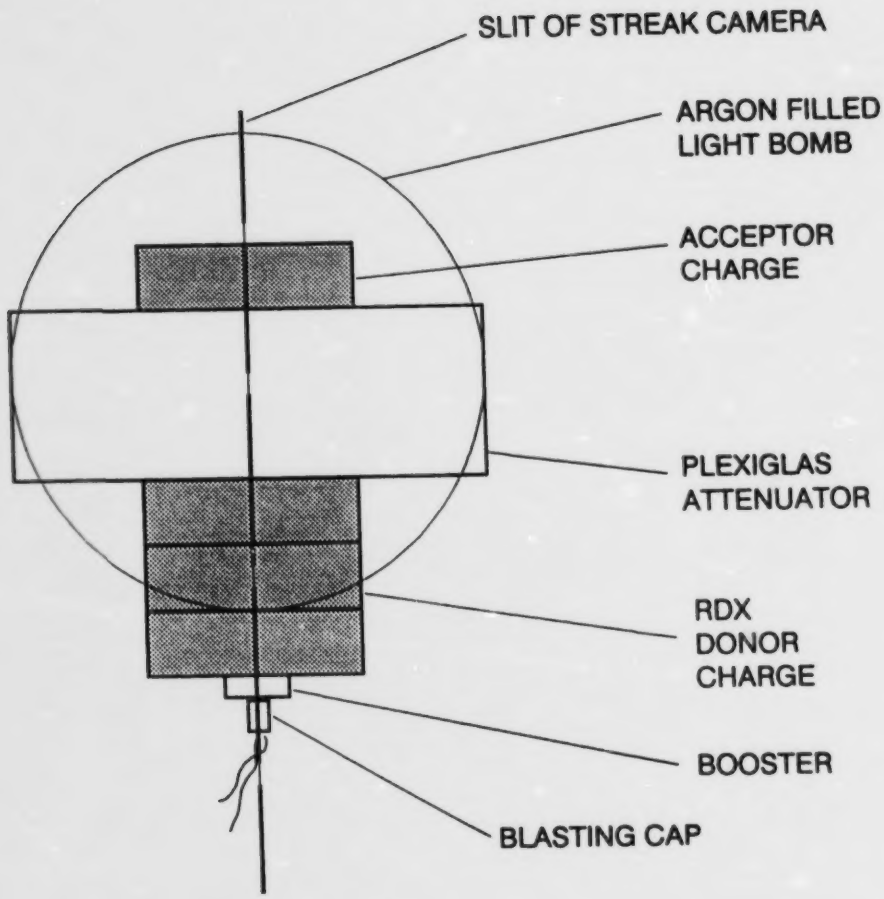

FIGURE 12: EXPERIMENTAL ARRANGEMENT FOR THE CALIBRATED GAP TESTS.

wave reaches the free surface of the acceptor it moves it, producing a cutoff of light. From the slope of this line the free surface velocity can be measured. If the acceptor detonates a bright flash is normally seen in the streak camera record.

Typical results are shown in Figures 13, 14, 15, 16 and 17.

2.4 *Interpretation of the Experimental Results*

The results of the calibrated gap test are reported as free surface velocity - impact pressure curves which indicate the thresholds to reaction and detonation. In order to obtain these curves it is necessary to have the relationship between pressure in the plexiglas attenuator and the thickness of the attenuator for the case of the shocks provided by the standard donor. From the streak camera records the shock velocity in the plexiglas can be obtained at various points of the attenuator. The relationship between shock velocity and thickness is shown in Figure 18 . From the shock velocity and the Hugoniot of the plexiglas the particle velocity can be calculated.

The Hugoniot of the plexiglas can be expressed as[10]:

$$U_s = 2430 + 1.5785\, U_p \qquad (2.1)$$

where U_s is the shock velocity (m/sec) and

U_p is the particle velocity (m/sec)

The pressure in the plexiglas can be calculated from the well known relationship

$$P = \rho\, U_p U_s \qquad (2.2)$$

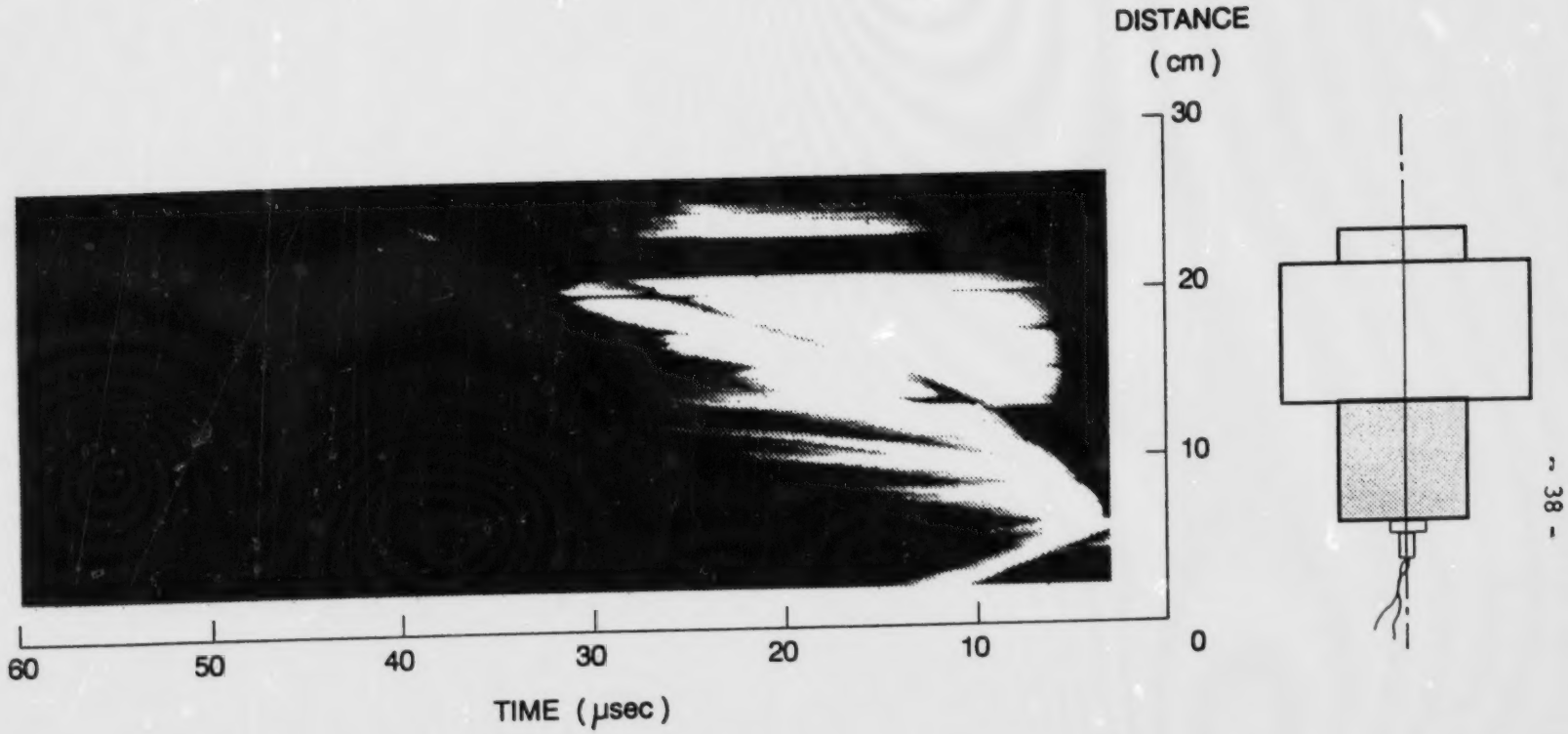

FIGURE 13: TYPICAL STREAK CAMERA RECORD FOR THE CASE OF DETONATION OF THE ACCEPTOR.

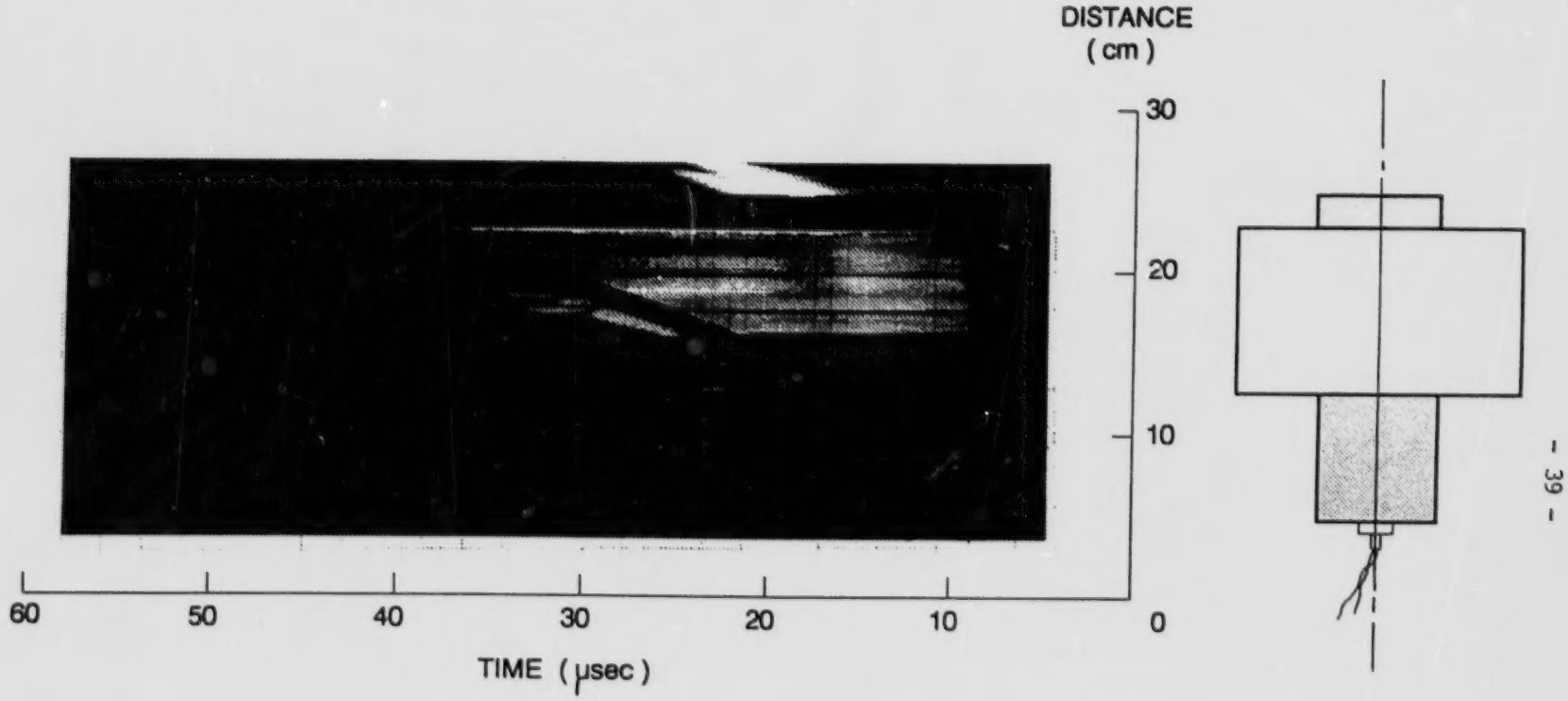

FIGURE 14: STREAK CAMERA RECORD OF THE CALIBRATED GAP TEST FOR WAXED RDX.

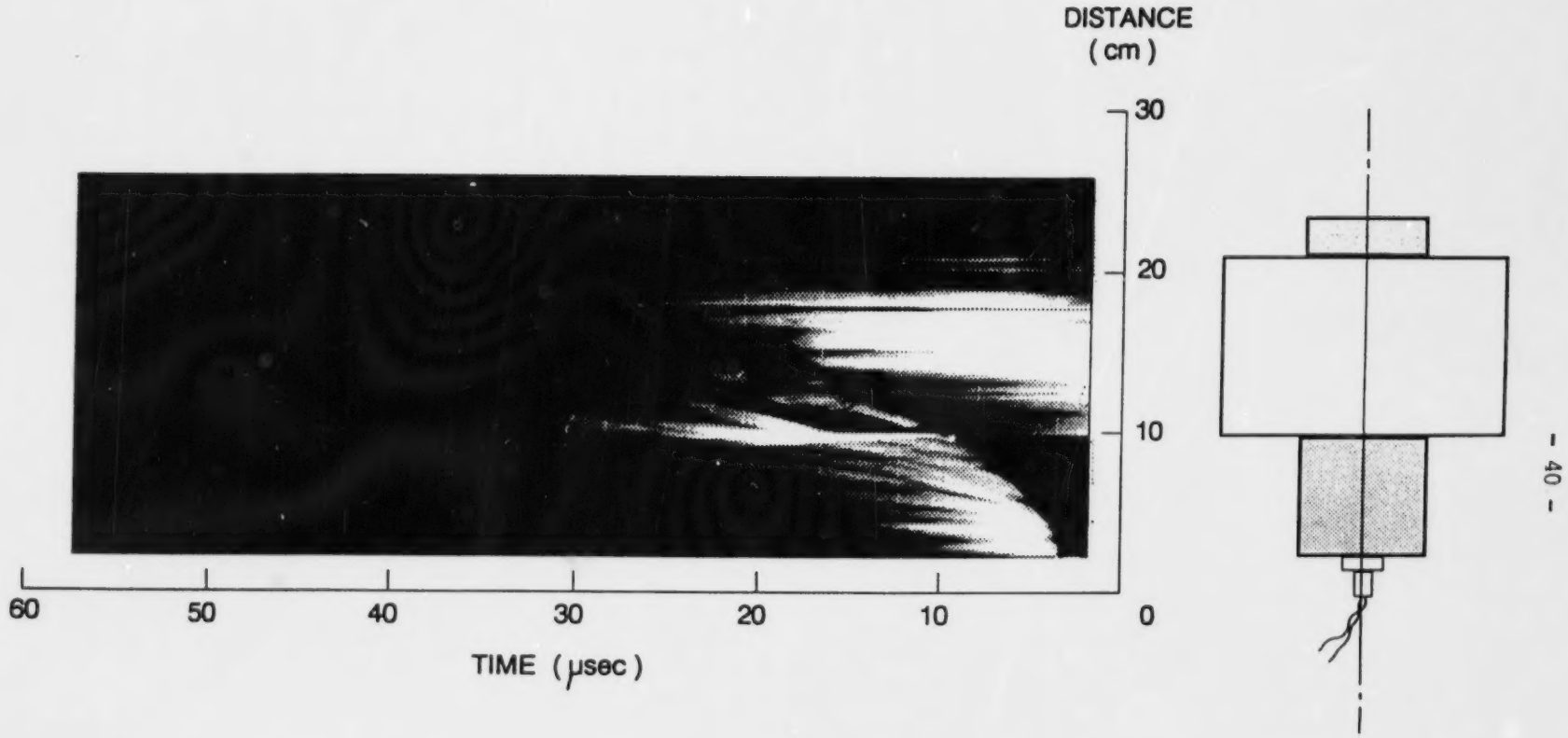

FIGURE 15: STREAK CAMERA RECORD OF THE CALOBRATED GAP TEST FOR WAXED RDX.

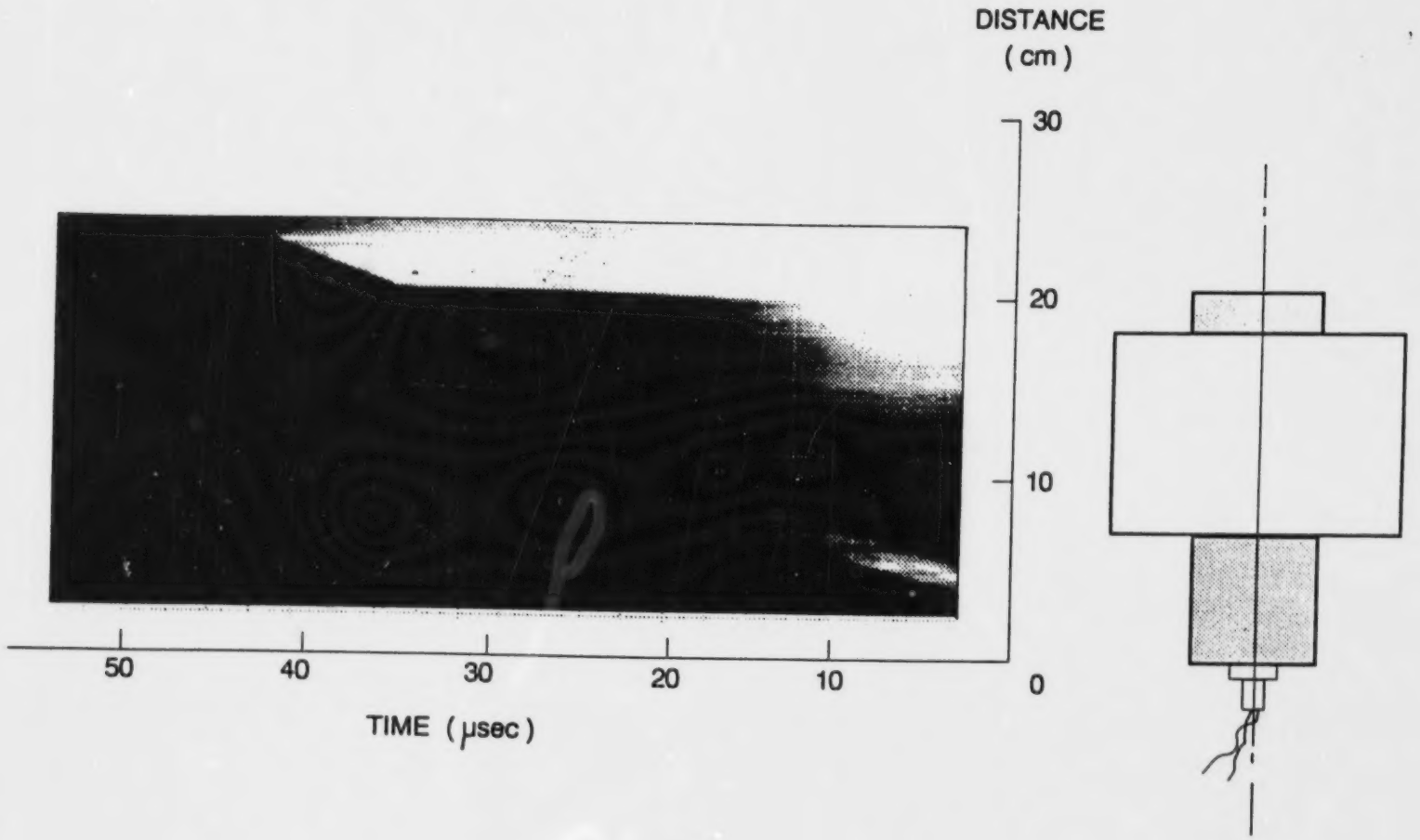

FIGURE 16: STREAK CAMERA RECORD OF THE CALIBRATED GAP TEST FOR SLURRY A.

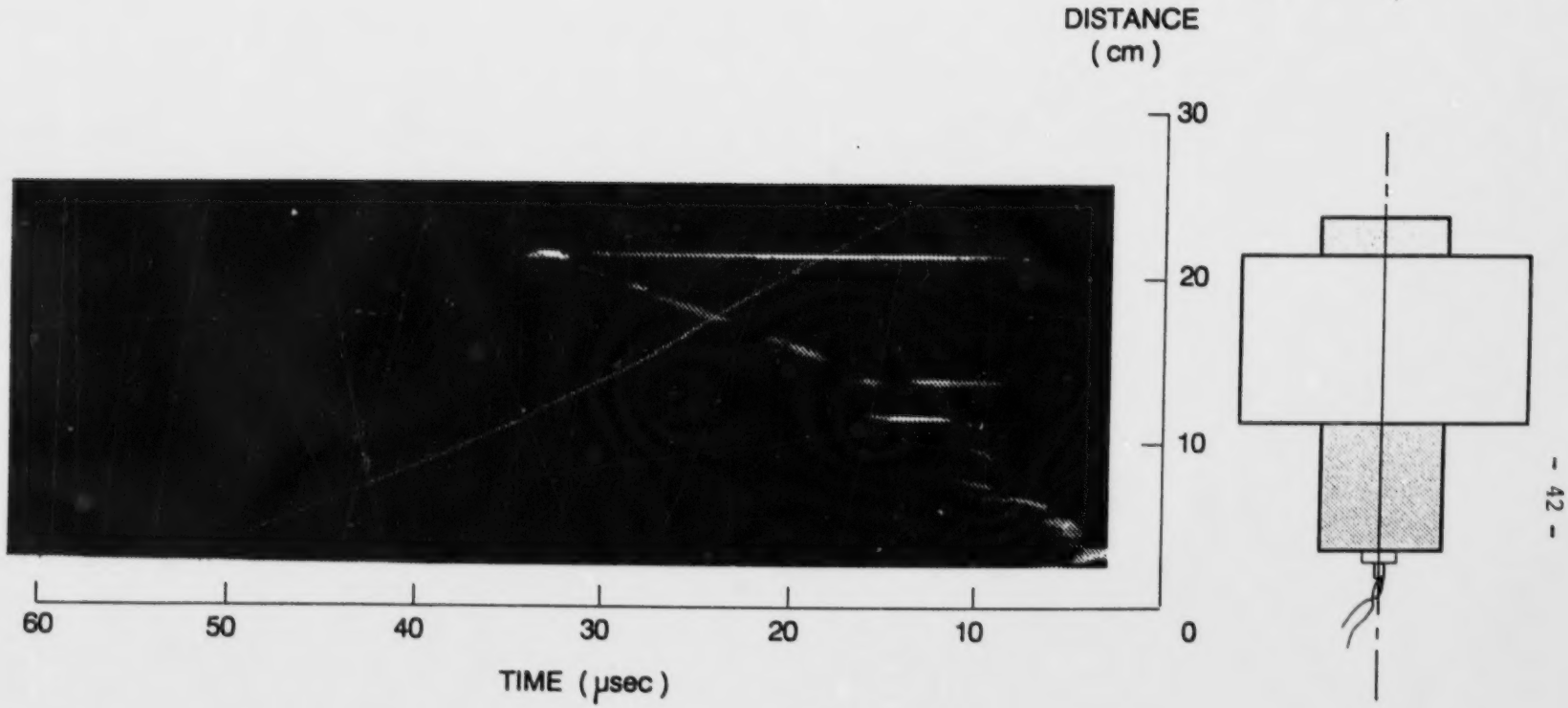

FIGURE 17: STREAK CAMERA RECORD OF THE CALIBRATED GAP TEST FOR EMULSION A.

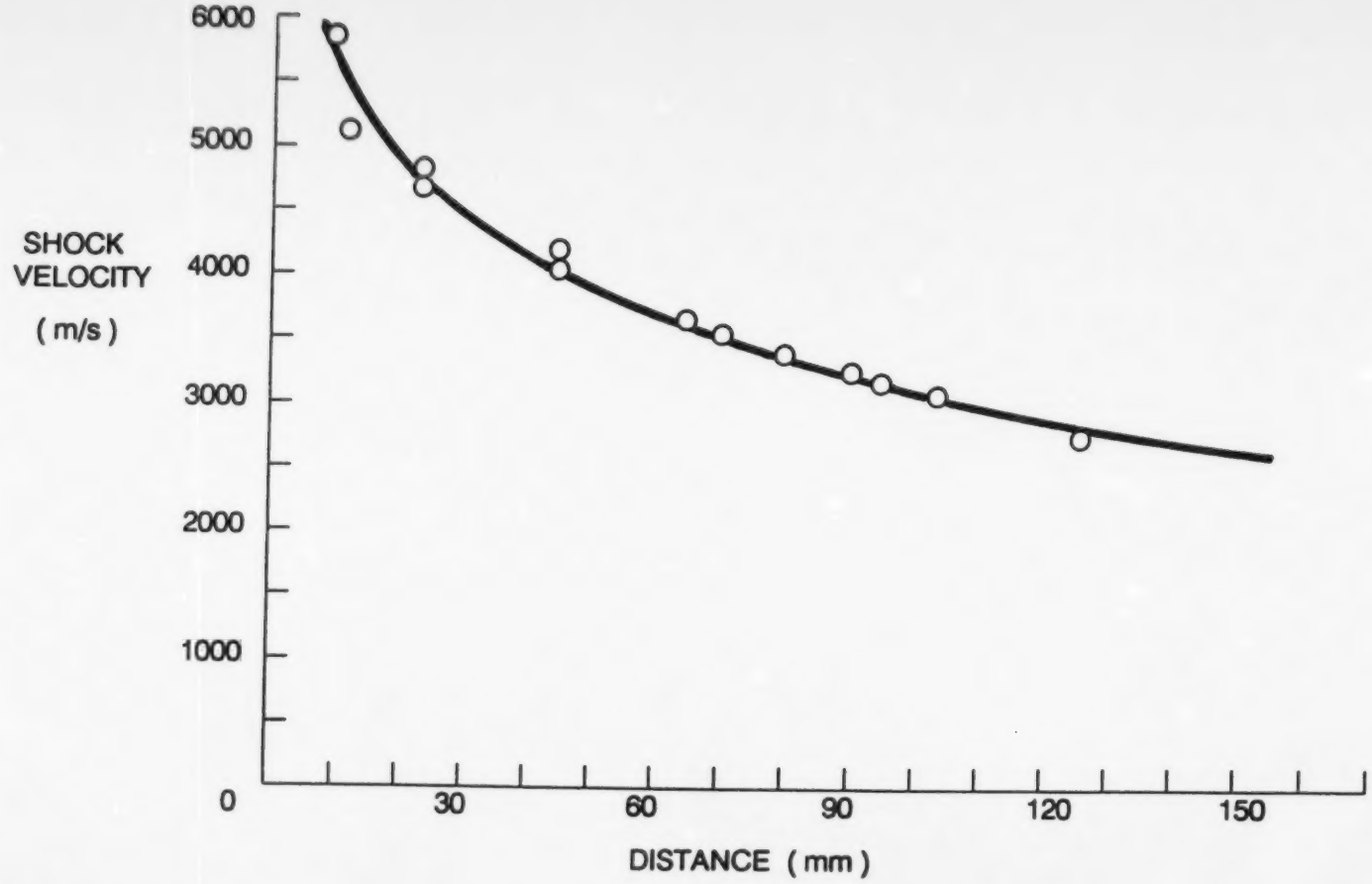

FIGURE 18: SHOCK VELOCITY VERSUS PLEXIGLAS THICKNESS FOR THE CALIBRATED GAP TEST.

where ρ is the density of the plexiglas.

The relationship between pressure in the plexiglas and the plexiglas thickness is shown in Figure 19.

The initial pressure in the explosive can be calculated if the Hugoniot of the unreacted explosive is known. It is assumed that the flow is one dimensional and that the pressure at the interface where the shock enters the explosive is changing slowly with time. These assumptions are not exactly correct but no alternative is available at the present time. Furthermore it is assumed that the pressure and particle velocity are the same on both sides of the attenuator - explosive interface. The particle velocity of the attenuator can be found by determining the Hugoniot of the attenuator and the relationship between shock velocity and attenuator thickness for the given experimental system as explained previously. Since the shock pressure and the particle velocity in the attenuator are known, the pressure P and the particle velocity U_p in the explosive are found by reflecting the attenuator Hugoniot along the line U_p = constant, and finding the intersection of this curve and the line provided by the Hugoniot of the explosive. The process is illustrated in Figure 20.

Normally Hugoniots of explosives are obtained by performing wedge tests. However wedge tests are expensive and difficult to perform. In a few cases it is reasonable to estimate Hugoniots of the explosives under study. In the numerical modelling part of the present study, Hugoniots were estimated based on values obtained by previous work[23] and on values available in the literature[30]. The experimental results here are reported as relationships between plexiglas shock pressure and free surface

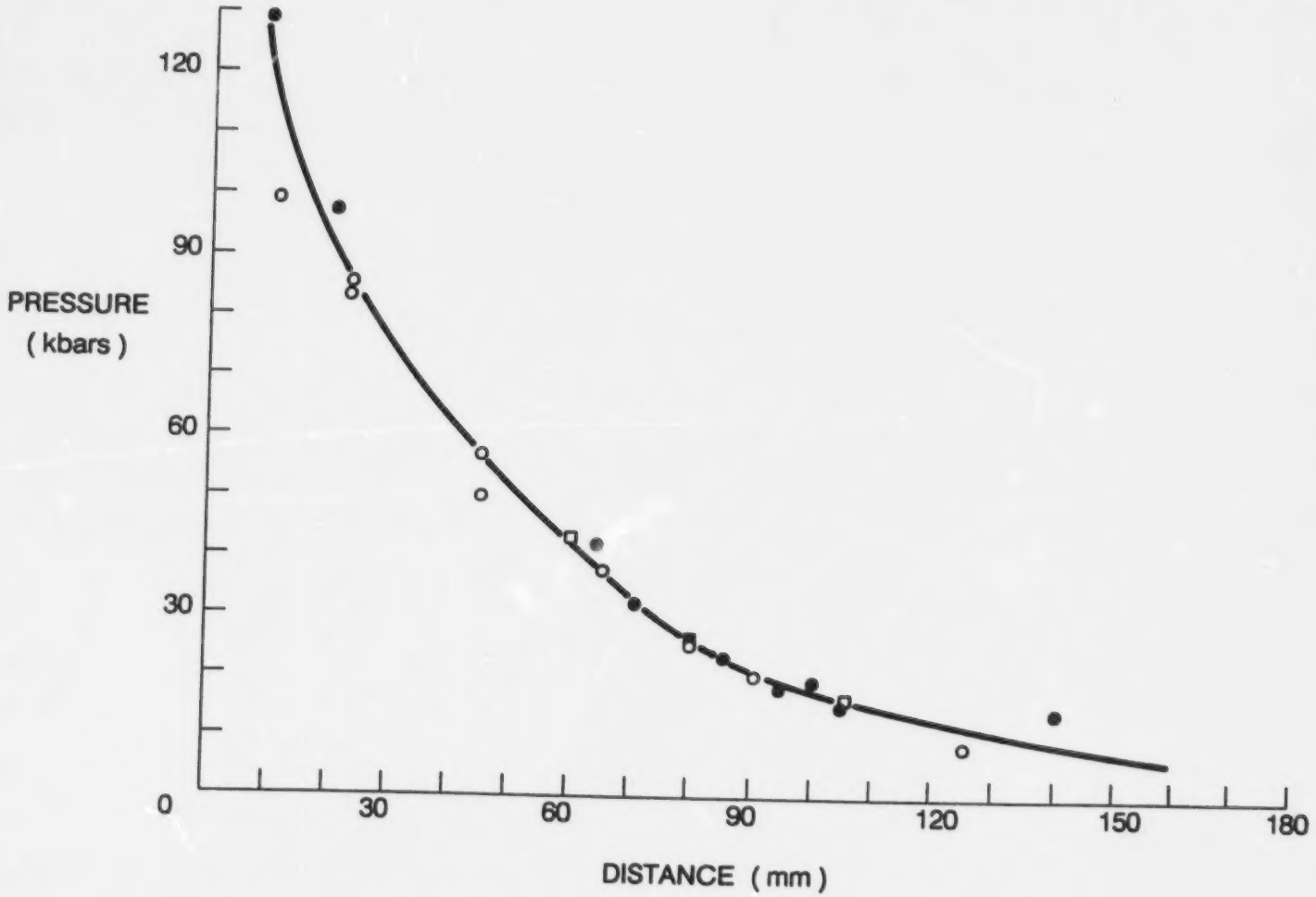

FIGURE 19: ATTENUATION OF THE SHOCK WAVE PRODUCED BY THE DONOR IN THE CALIBRATED GAP TEST.

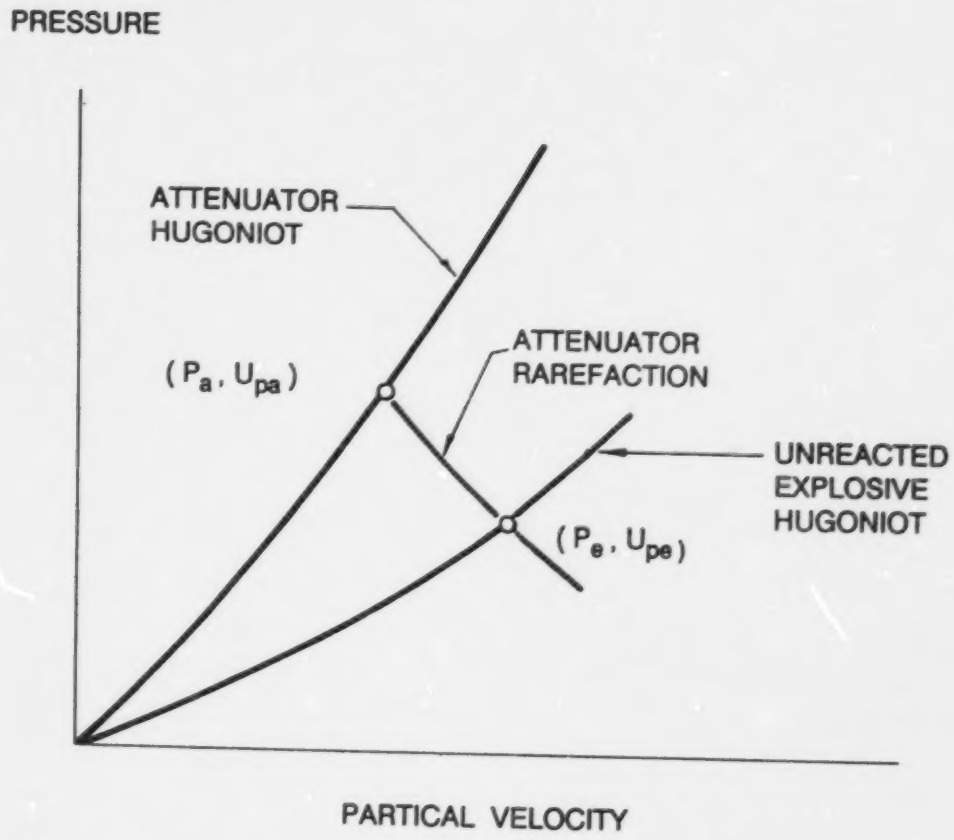

FIGURE 20. GRAPHICAL METHOD OF OBTAINING SHOCK PRESSURE AND PARTICLE VELOCITY IN UNREACTED EXPLOSIVE.

velocity of the acceptor charge.

The free surface velocity of the acceptor is twice the particle velocity at the free face of the acceptor. The Hugoniot of the unreacted explosive is given by the relationship,

$$U_s = C + S\,U_p \qquad (2.3)$$

where U_s is the shock velocity

U_p is the particle velocity and

C and S are constants.

From the momentum conservation equation,

$$P_i = \rho\,U_s U_p \qquad (2.4)$$

where P_i is the pressure

ρ is the initial density

U_s is the shock velocity and

U_p is the particle velocity.

From (2.3) and (2.4),

$$P_i = \rho\,(\,C + S\,U_p\,)\,U_p \qquad \text{or}$$

$$P_i = \rho\,C\,U_p + \rho\,S\,U_p^{\,2} \qquad (2.5)$$

Let us assume that the pressure in the plexiglas, at the interface between plexiglas and explosive is related to the pressure inside the unreacted explosive by the relationship,

$$P = P_i\,e^{-\alpha x} \qquad (2.6)$$

where P is the pressure inside the unreacted explosive

P_i is the pressure inside the plexiglas plate, at the interface between plexiglas and explosive

x is the distance between the plexiglas/explosive interface and the point of interest in the acceptor explosive and

α is a constant dependant on the particular system which expresses the attenuation of the shock wave inside the acceptor.

For example in the case of the wave in the plexiglas attenuator the above expression becomes,

$$P = 141.5\ e^{-0.2082x} \qquad (2.7)$$

where P is in Kbar and x in cm.

From equations (2.5) and (2.6)

$$P_i = (\rho C U_p + \rho S U_p^2)\ e^{-\alpha x}$$

Therefore

$$\frac{dP_i}{dU_p} > 0 \text{ and } \frac{d^2P_i}{dU_p^2} > 0.$$

Thus the function $P_i = f(U_p)$ is a rising function of U_p and it is concave up. The relationship between P and U_p is graphically shown in Figure 21. A typical experimental curve is also shown in the same Figure. A departure from the theoretical curve towards higher particle velocities at the same initial pressure will produce a point of inflection in the curve expressing the relationship between P_i and U_p. This can only be explained by the ignition of the sample due to the shock wave.

This point can be found easily if a significant amount of reaction takes place suddenly so that there is a sudden change of the P-U_p relationship. If this change is gradual the threshold point can be more difficult to obtain. In these cases a large number of experiments might be necessary.

2.5 *Results*

Three explosives were tested by the above technique to obtain the thresholds to ignition. These explosives were waxed RDX (90% RDX, 10% wax) at a density of 1.6g/cc, Slurry A and Emulsion A.

The waxed RDX was pressed to the required density (5000 psi) by using a hydraulic press. It was used as a standard because of the reproducibility of the acceptor charges. The slurry and the

FIGURE 21: PRESSURE-PARTICLE VELOCITY RELATIONSHIP FOR UNREACTED AND REACTIVE EXPLOSIVE

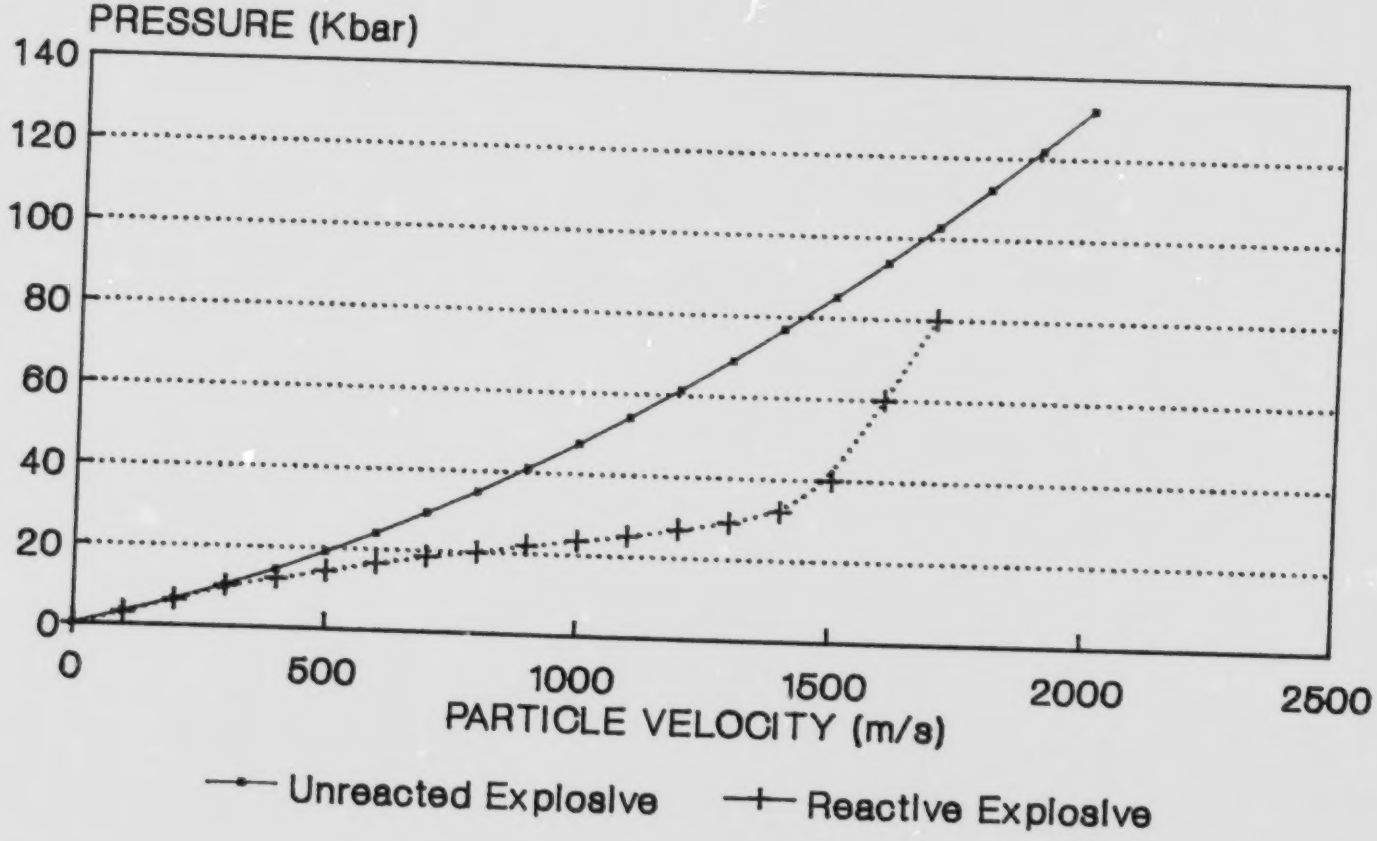

emulsion products were typical cap sensitive commercial compositions. Both of them are used in small diameter applications and they contain a small amount of Aluminum (less than 5%).

The slurry uses air bubbles in order to achieve the desirable sensitivity. These air bubbles vary in size from a few microns to a few millimetres.

The emulsion uses glass microballoons with an average size of 70 microns. The pressure of the gas inside the microballoons is normally below the atmospheric pressure.

Further differences in the two products are found in their physical characteristics. In the slurry the discontinuous phase consists of fuels and oxidizer salt crystals and the continuous phase is the oxidizer solution. In the emulsion the continuous phase is the oil while the discontinuous phase consists of the oxidizer salt solution. There are no crystals in the emulsion and the mix is much more intimate than in the case of the slurry.

2.5.1 *Pressed RDX (ρ = 1.6g/cc)*

The experimental results for pressed RDX are shown in Table 2. Figure 22 shows the relationship between the free surface velocity of the acceptor and the thickness of the plexiglas attenuator. Figure 23 shows the relationship between the acceptor free surface velocity and the shock pressure in the plexiglas at the interface between attenuator and acceptor. It follows that the ignition threshold (for the developed donor) is at a plexiglas thickness of 115-125mm or at a shock pressure in the plexiglas between 11 and 13Kbar.

TABLE 2: EXPERIMENTAL RESULTS FOR WAXED AND PRESSED RDX

ATTENUATOR THICKNESS (mm)	ACCEPTOR FREE SURFACE VELOCITY (m/sec)
155	330
118	480
118	510
110	890
105	990
105	1270
100	1800
95	DETONATION
89	DETONATION
89	DETONATION

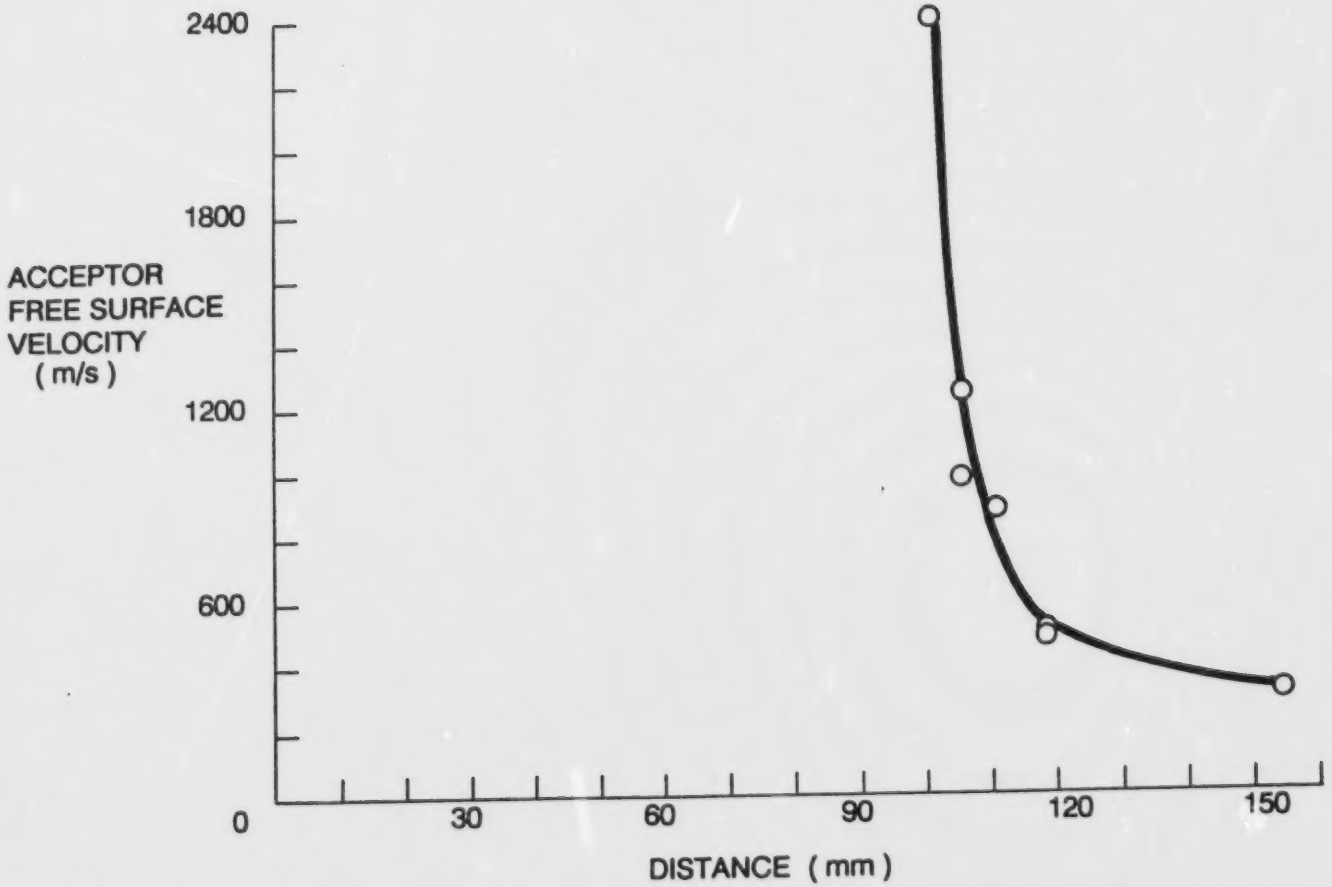

FIGURE 22: ACCEPTOR FREE SURFACE VELOCITY VERSUS PLEXIGLAS THICKNESS FOR WAXED AND PRESSED RDX.

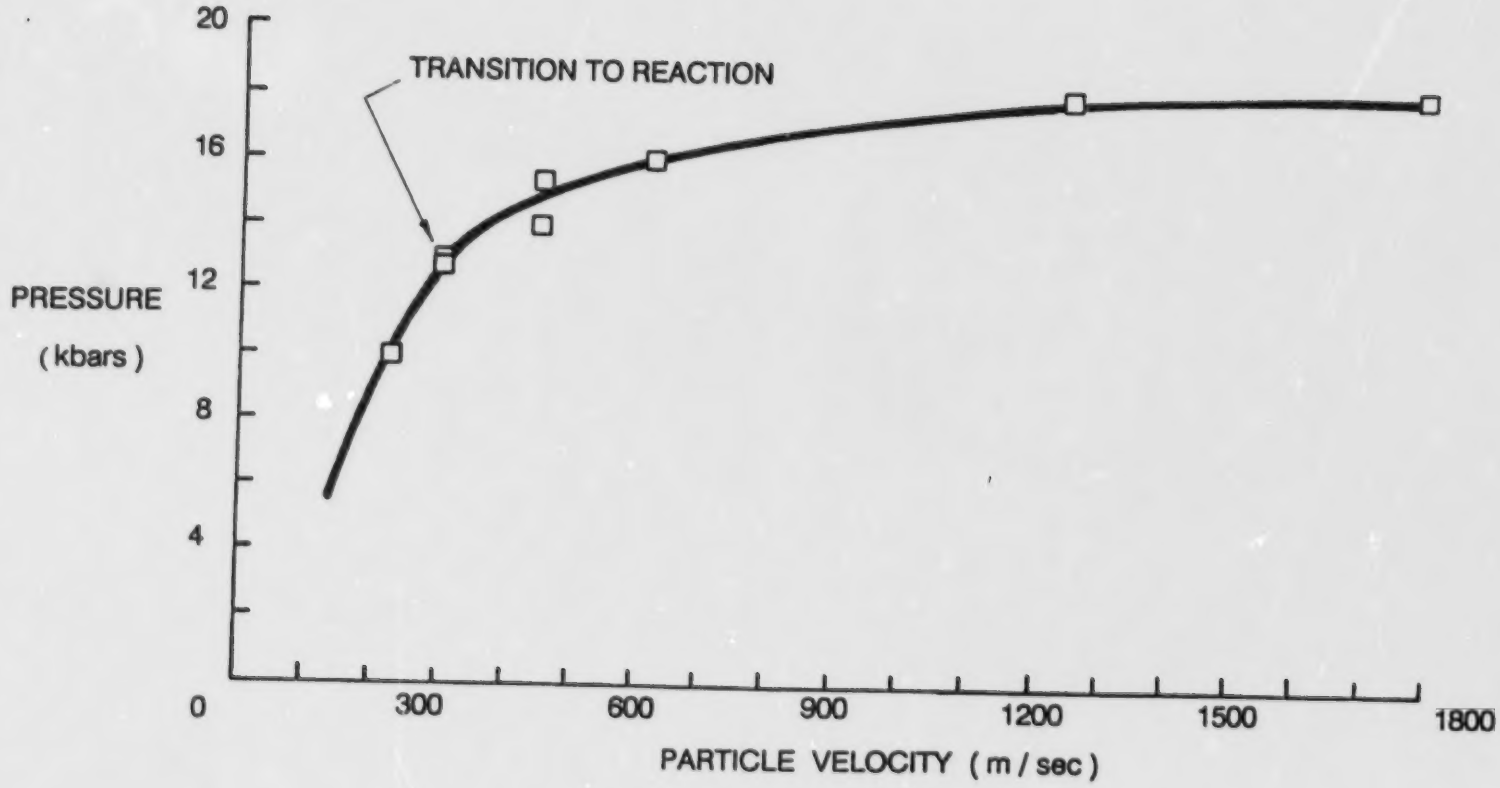

FIGURE 23: INITIAL PRESSURE VERSUS FREE SURFACE VELOCITY FOR WAXED AND PRESSED RDX.

2.5.2 *Slurry A (ρ = 1.15g/cc)*

The experimental results for slurry type A are shown in Table 3. Figure 24 provides the relationship between plexiglas thickness and slurry acceptor free surface velocity while Figure 25 illustrates the relationship between plexiglas shock pressure and acceptor free surface velocity. The ignition threshold is at a thickness of 135-145mm or at a shock pressure in the plexiglas between 10 and 12Kbars.

2.5.3 *Emulsion A (ρ = 1.15gcc)*

The experimental results are shown in Table 4. The results are plotted as plexiglas thickness - acceptor free surface velocity and plexiglas shock pressure - acceptor free surface velocity curves in Figures 26 and 27 respectively. The ignition threshold is at a thickness of 105 - 115mm or at shock pressure in the plexiglas of 13 - 15 Kbars.

2.6 *Discussion*

The experimental work shows that a threshold to ignition could be found in all three explosives tested. The slurry was proven to be the most sensitive of all. This agrees with the projectile tests which were conducted previously. However the results of the projectile tests are reported as detonations or

TABLE 3: EXPERIMENTAL RESULTS FOR SLURRY A

ATTENUATOR THICKNESS (mm)	ACCEPTOR FREE SURFACE VELOCITY (m/sec)
161	450
92	4450
104	3960
115	3670
132	1480
100	4000

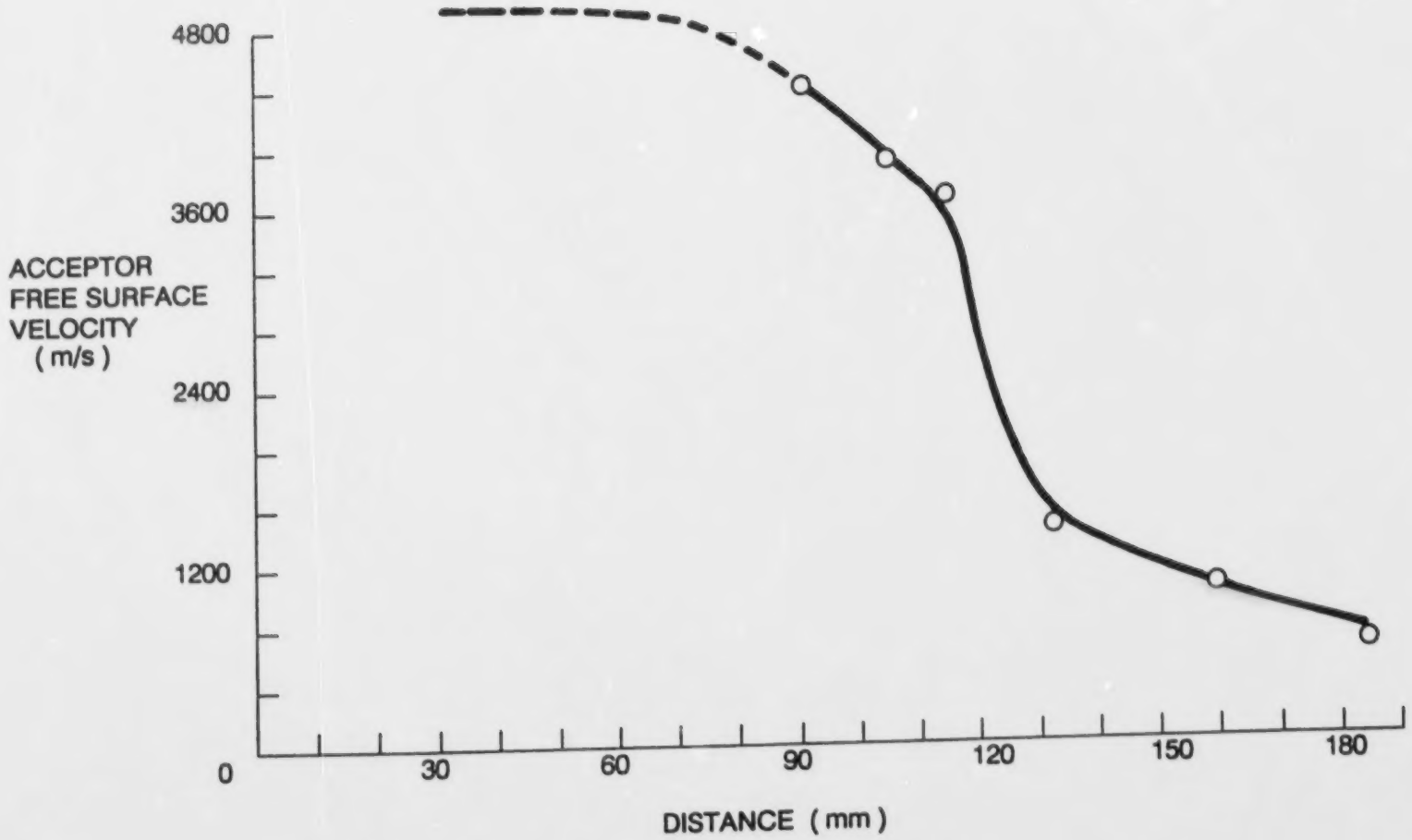

FIGURE 24: ACCEPTOR FREE SURFACE VELOCITY VERSUS PLEXIGLAS THICKNESS FOR SLURRY A.

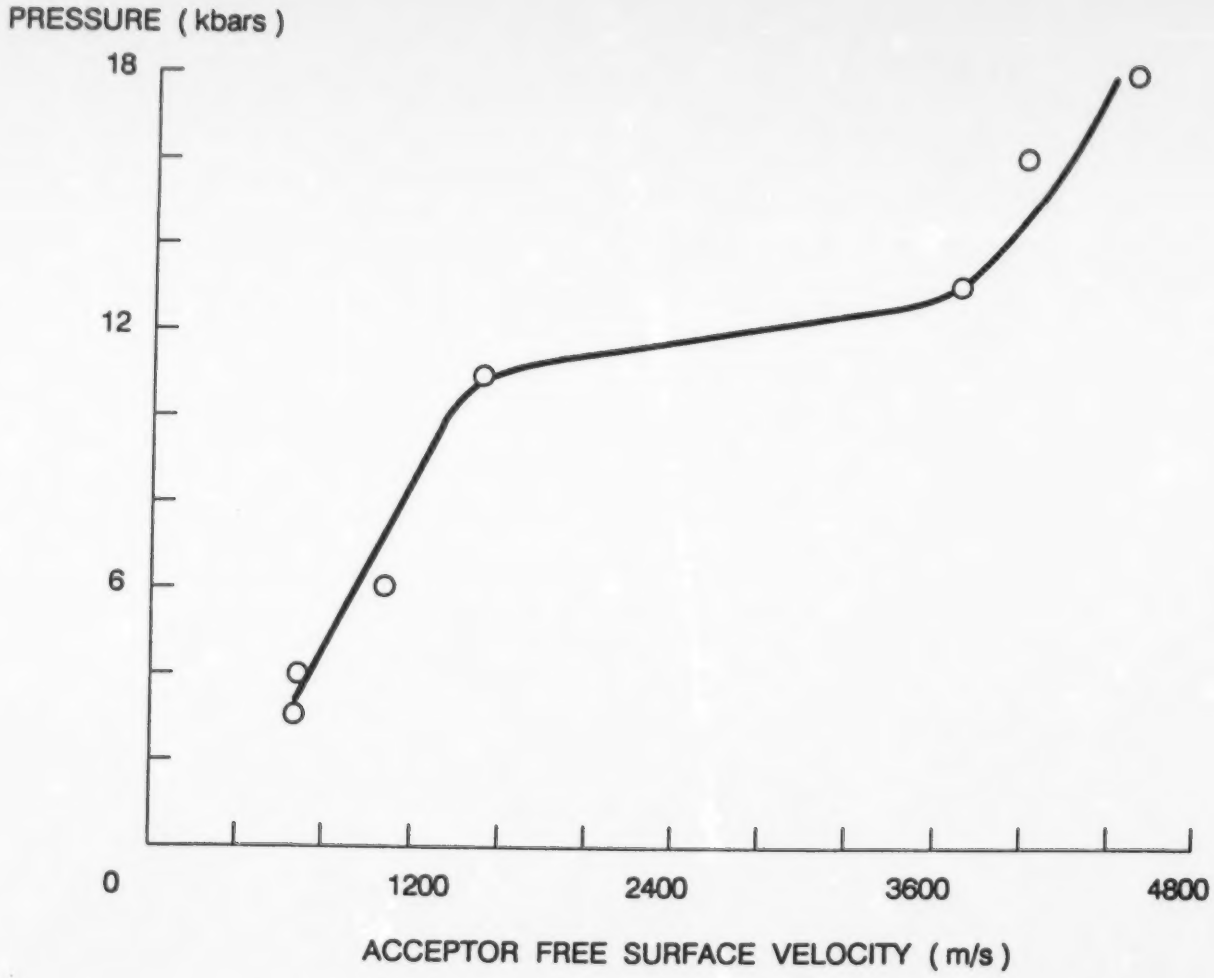

FIGURE 25: PRESSURE VERSUS FREE SURFACE VELOCITY FOR SLURRY A.

TABLE 4: EXPERIMENTAL RESULTS FOR EMULSION A

ATTENUATOR THICKNESS (mm)	ACCEPTOR FREE SURFACE VELOCITY (m/sec)
140	380
127	450
115	600
105	460
95	1100
80	5200
75	5800

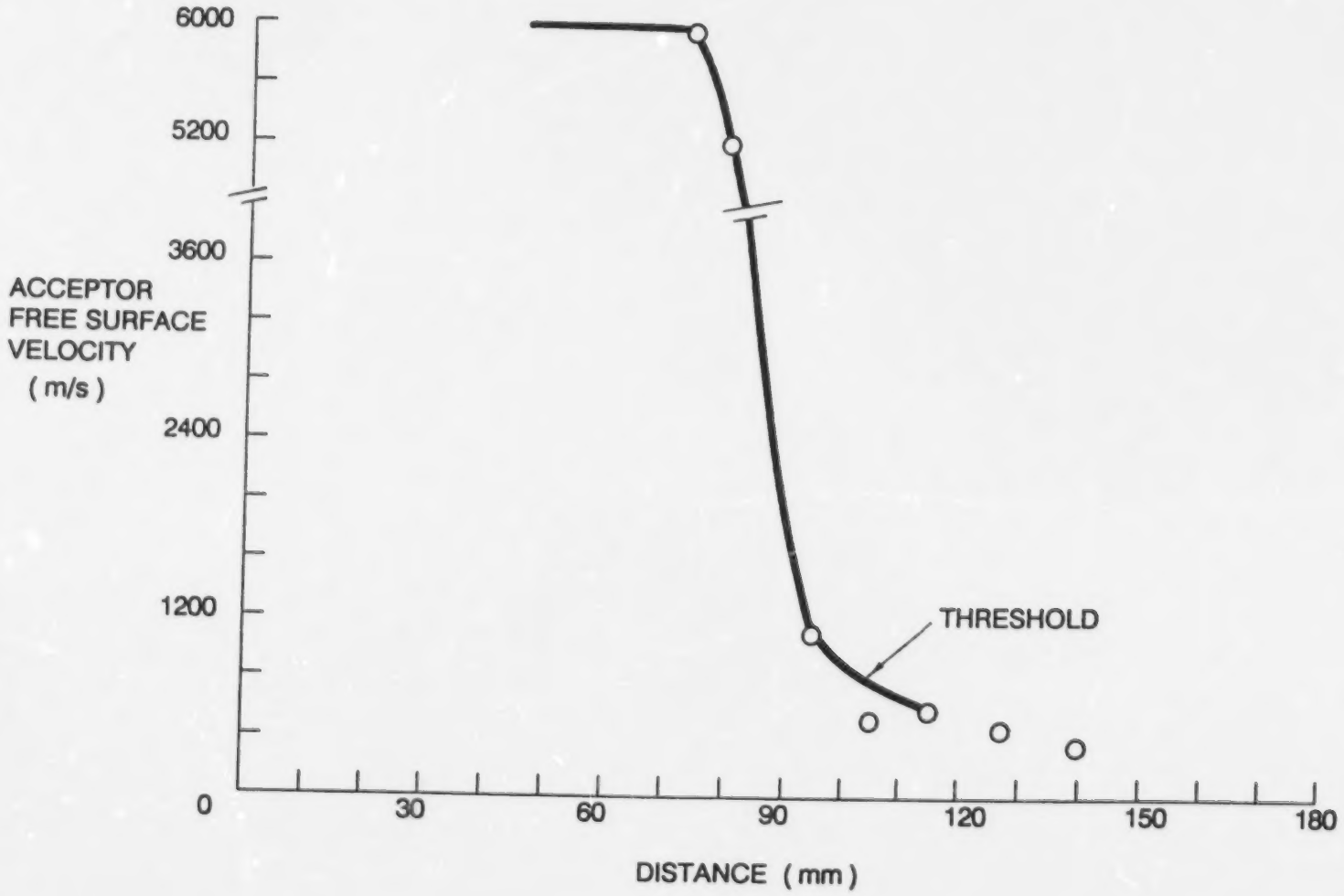

FIGURE 26: ACCEPTOR FREE SURFACE VELOCITY VERSUS PLEXIGLAS THICKNESS FOR EMULSION A.

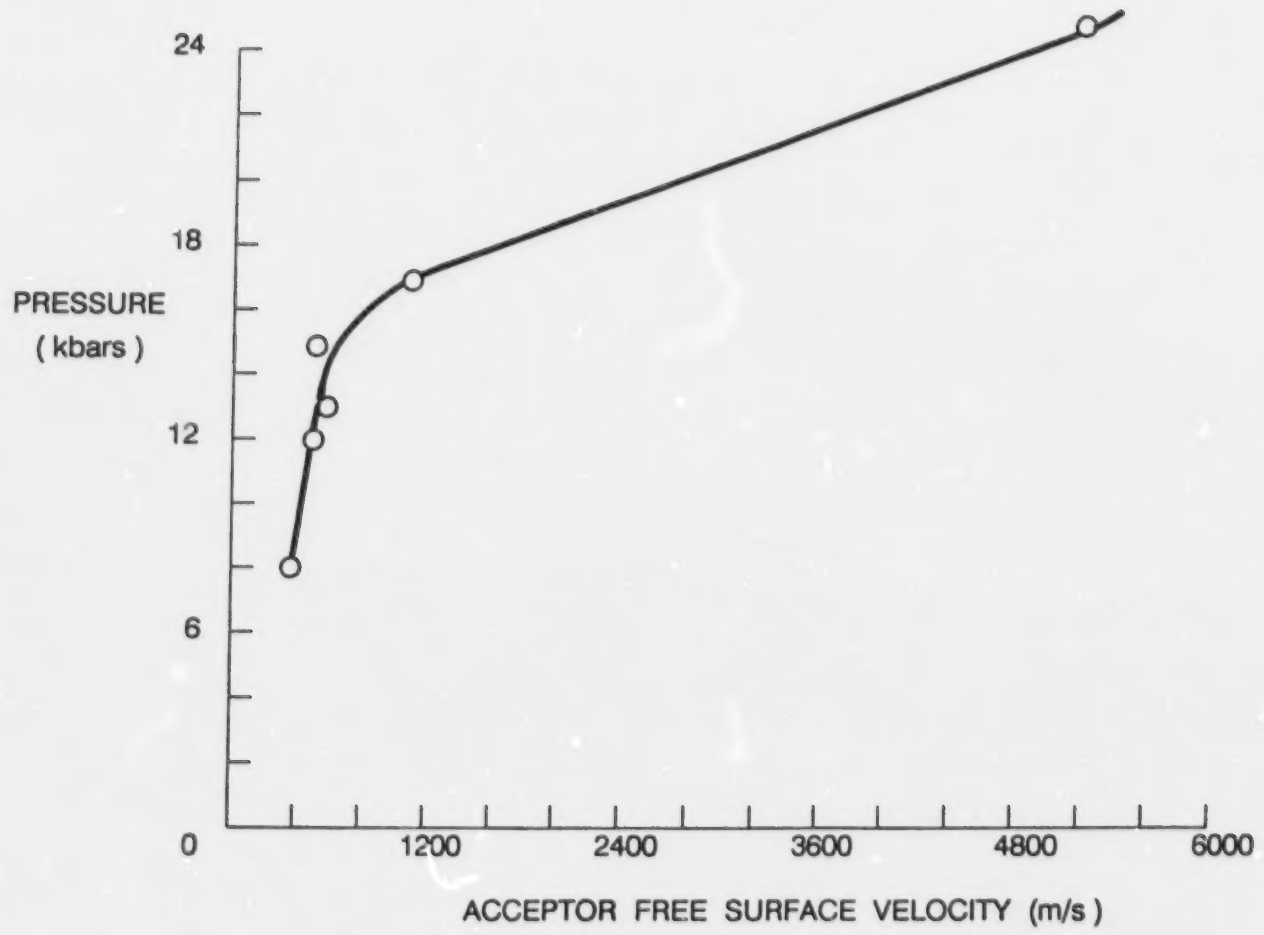

FIGURE 27: PRESSURE VERSUS FREE SURFACE VELOCITY FOR EMULSION A.

failures. Therefore any ignition which did not propagate to a detonation is reported as a failure. It is worth mentioning that the sensitivity of the slurry is based on gas bubbles which are dispersed in its mass.

Furthermore the slurry exhibited a larger area where the build-up of burning takes place. In this area the response of the explosive depends upon various parameters (confinement, size etc.) and can be detonative. Therefore in order to assess the sensitivity of the slurry one has to consider the impact pressure which results in the start of burning (threshold to burning in the previous curves). This pressure is different than the critical pressure for initiation. In the experiments conducted the difference in the pressures is of the order of 5-7 Kbars.

In addition to this, the extent of the zone where build up takes place shows that a significant amount of burning takes place before detonation occurs.

In the case of the waxed RDX and the emulsion a rapid build-up to detonation is observed when the pressure is increased above the threshold for burning.

In a few cases detonation was observed several microseconds after the arrival of the shock wave at the interface plexiglas/acceptor. Figure 28 shows a streak camera record illustrating this. The acceptor detonated about 60 μsec after impact. The detonation is indicated by the brilliant air shock which is produced.

This event was recorded for emulsion type A. However it was more common in the experiments conducted for the slurry. This might be an indication of the role of air bubbles in the sensitivity of the slurry explosive. It seems that adiabatic

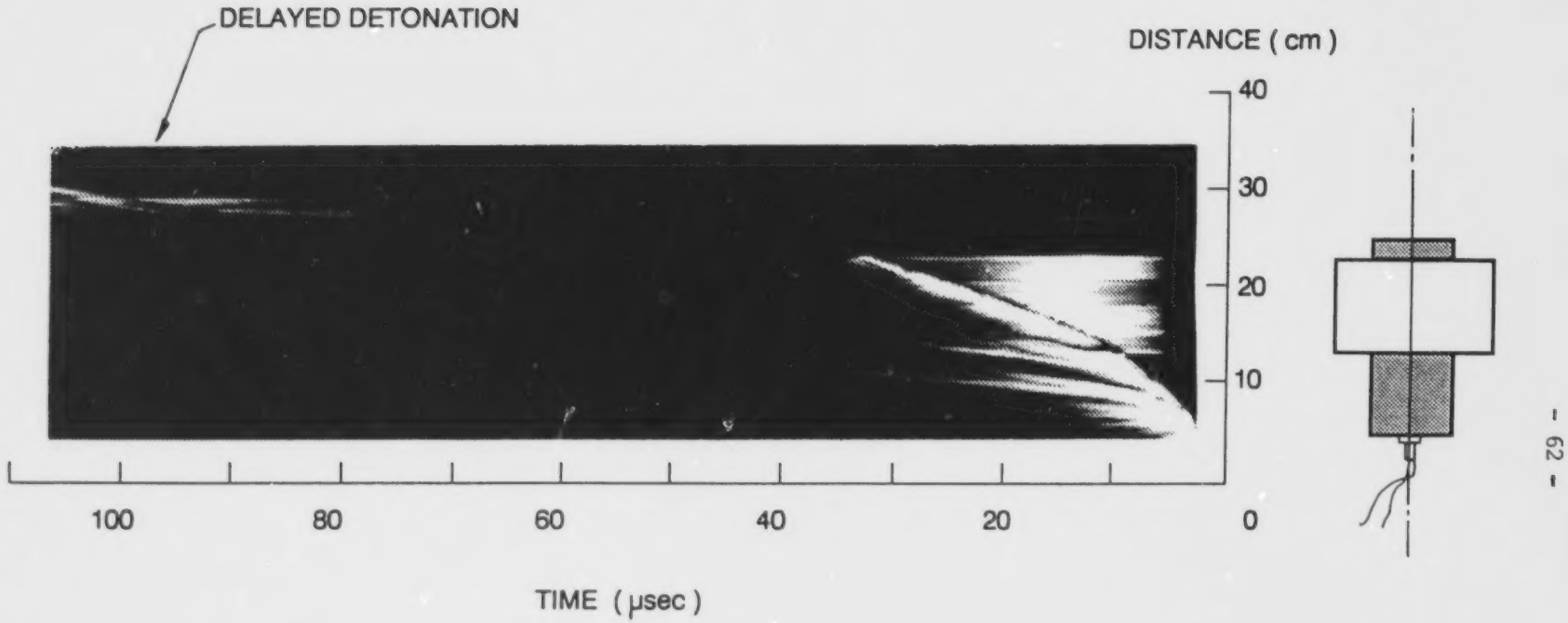

FIGURE 28: STREAK CAMERA RECORD FOR EMULSION A WHERE

compression of the entrapped gas bubbles can contribute to the initiation of the commercial explosives by a low amplitude shock wave. The time from impact to detonation is sufficiently long to make heat conduction possible.

3.0 *NUMERICAL MODELLING OF THE GAP TEST*

3.1 *Introduction*

The previously reported values of the critical pressures for burning are dependant not only on the chemical composition and the physical properties of the acceptor charge, but also on the dimensions of the tests. A donor of different dimensions will produce different impulses and an acceptor of a different diameter will also change the pressure -time profile inside the acceptor charge. Obviously, the threshold values given represent only the test described previously. As such the test is good only for comparative purposes. In order to obtain values which are not dependant on the geometry, the pressure profile has to be considered. This can be performed by calculating the critical energy for the start of burning.

Critical energies were calculated by using program GAP which is based on the 'HYDREL' code[7] and the 'TROTT'[24] code. The basics of the GAP code and the results of the calculations are presented in the following.

3.2 *The Hydrodynamic Calculations*

The hydrodynamic calculations are based on the code TROTT written by Seaman[24]. In order to start the calculations the materials of the problem are divided into small elements by means of a grid. A typical grid describing the gap tests is shown in Figure 29. The computations proceed forward in time in small

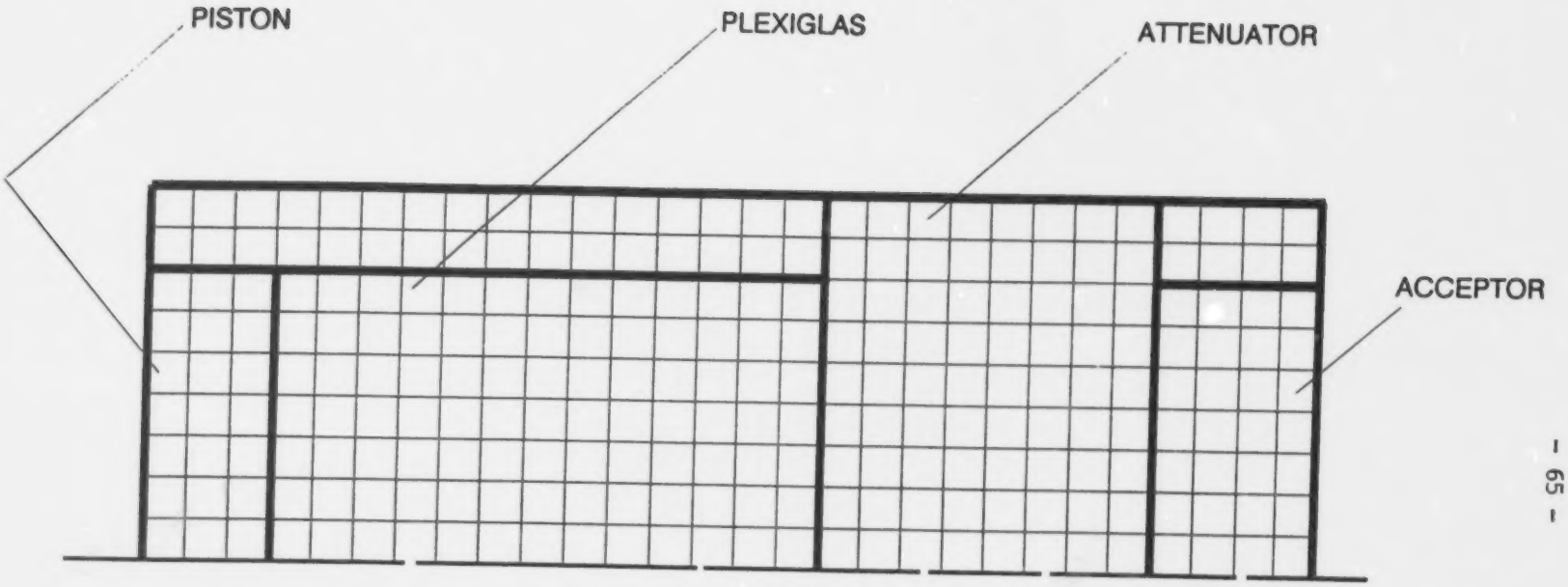

FIGURE 29: TYPICAL GRID DESCRIBING THE GAP TESTS.

increments. At each increment, calculations are made of stresses, velocities, displacements and energies at each cell and coordinate point[24]. A simplified flow chart of the program is shown in Figure 30.

Velocities and displacements, which are coordinate quantities, are defined at cell boundaries at full or half time increments. Other quantities, such as stresses, are defined at cell midpoints[24]. The approach taken is shown in Figure 31, which shows the cell quantities on a time-distance plot[24]. For simplicity only the Lagrangian direction J is shown.

The momentum calculation is used to determine velocity changes[24]. For example, the stresses, σ, in adjacent cells at the time step n, determine the forces on the mass centered at the point (j,n). Therefore, from the calculation

$$F = m\ a$$

where F is the force

m is the mass of the cell

a is the acceleration of the centre of the cell at the time step n, the acceleration is known. The acceleration of the mass at (J,n) determines the change in velocity from $X'_{(n-1/2)}$ to $X'_{(n+1/2)}$. From the new velocity, the coordinate position X at the time step n+1 is known[21].

Since the coordinate positions at time n+1 are known, the strains and density can also be calculated. The stresses at time step n+1, s, are obtained from the strains and the density using the constitutive relations[24].

The procedure is continued to the right through each cell for each time increment. The process is repeated until the time has reached the duration of interest.

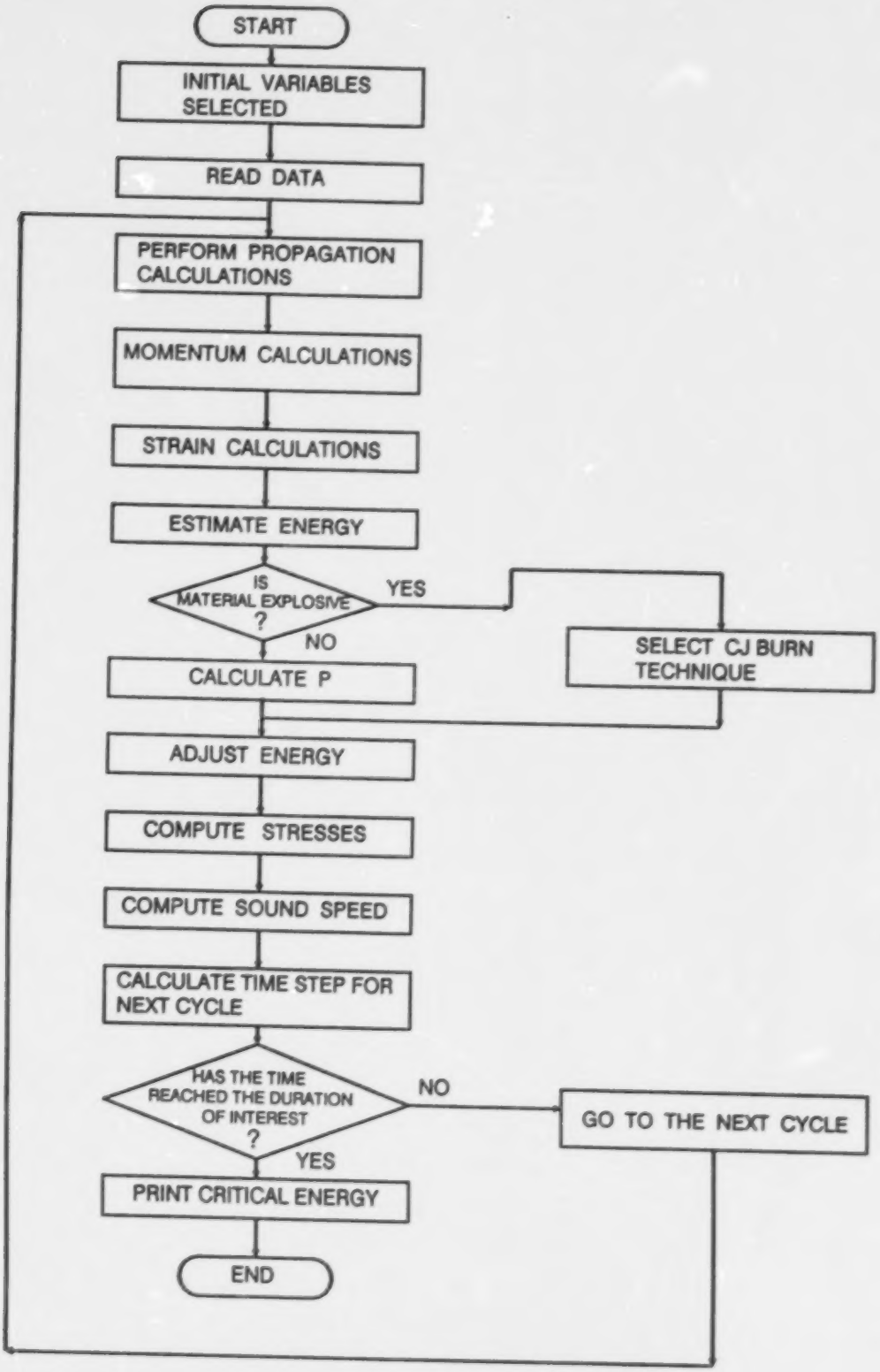

FIGURE 30: SIMPLIFIED FLOW CHART OF THE "GAP" COMPUTER CODE.

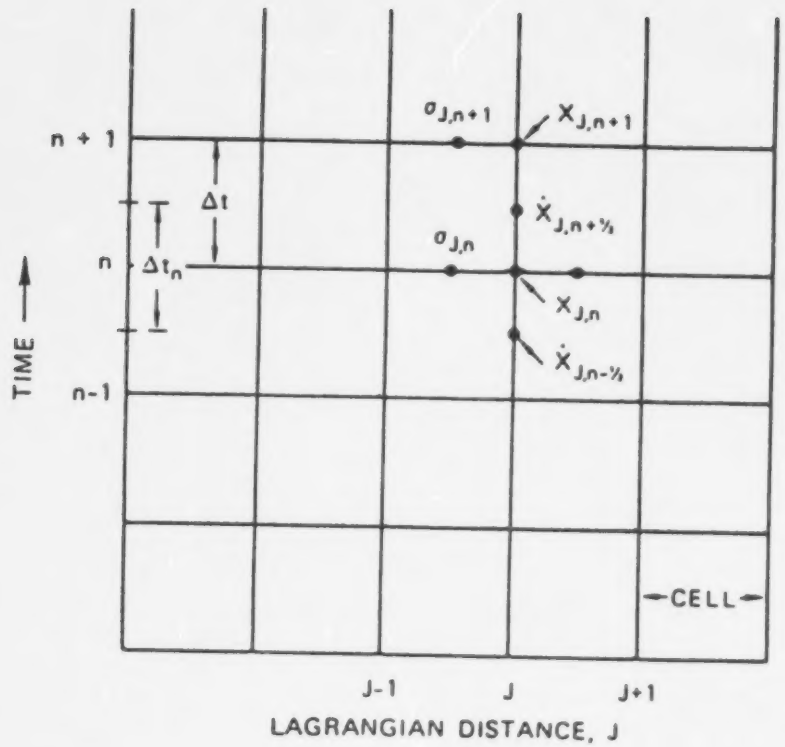

FIGURE 31: FINITE DIFFERENCE GRID SHOWING LOCATIONS OF VARIABLES USED IN THE MOMENTUM CONSERVATION RELATIONS.

In the model mass is conserved by using Lagrangian cells, which maintain a constant mass throughout the event.

Momentum conservation relations are used to obtain coordinate motions. In deriving the momentum conservation relations force balances around a finite element are considered[24].

The energy conservation relations are used for the calculation of the internal energy at each time step. The conservation of energy is expressed as[24]:

$$E^1 = E^\circ + V \sum_{ij} \sigma_{ij}\, d\varepsilon_{ij} \qquad (3.1)$$

Here E^1, E° are the internal energies at the end and at the beginning of the time increment,

V is the specific volume,

σ_{ij} is the stress and

ε_{ij} is the strain value at point ij.

The energy is calculated twice in the program. The first calculation follows the calculation of the density, while the strain and the stresses are those of the previous step. Then the stresses are computed based on the calculation and the energy is calculated again. The values of the energy which are obtained by the second calculation are stored so that they are used in the next cycle of calculations[24].

3.3 *The Pressure Models*

The stress tensor is separated into a pressure and a deviator tensor. The pressure is the average stress

$$P = 1/3 \sum_{ij} \sigma_{ij} \qquad (3.2)$$

The stress deviator elements are[24]

$$\sigma_{ij} = s_{ij} - P\delta_{ij} \qquad (3.3)$$

where σ_{ij} are stress tensor elements and δ_{ij} is the Kronecker delta[24].

The pressure is given as a function of the internal energy, the density and the mass fraction of the solid components of the material. It is calculated by the HOM equation of state[10,25]. The HOM equation of state can be used for both reactive and non reactive materials. Obviously, in the case of non reactive materials, the fraction of solids is always equal to 1. In the case of reactive materials the fraction of the solids depend on the decomposition rate given by the reactive model.

3.4 *The Model for the Donor Charge*

The C-J burn technique was used for the reactive model of the donor charge. According to this technique the fraction of undecomposed explosive varies linearly between the initial volume and the C-J volume. Thus:

$$W = \frac{V - V_{CJ}}{V_0 - V_{CJ}} \qquad (3.4)$$

where W is the fraction of undecomposed explosive,

V is the specific volume of the explosive,

V_0 is the initial specific volume of the explosive

and

V_{CJ} is the specific volume of the explosive at the detonation state.

The specific volume at the detonation state is calculated by using a thermohydrodynamic code. In the present case the specific volume was calculated by using TIGER[26].

Decomposition starts as a result of the impact by a piston. The initial velocity of the piston was assumed to be equal to the particle velocity at the detonation state. This particle velocity is calculated by TIGER.

3.5 *The Model for the Attenuator*

The attenuator was assumed to behave as a fluid. This assumption is justified because the yield strength of plexiglas is low compared to the shock pressures provided by the donor explosive.

3.6 *The Artificial Viscosity*

It has been found that significant oscillations can occur in the cell quantities after the passage of a shock wave . These oscillations do not have a physical meaning[24,25,27,28].

In view of this problem, an artificial viscous stress is commonly used in the finite difference propagation calculations. Thus, all the shocks are broadened on the difference mesh and the entire flow field can be treated by the conservation equations of the continuous flow[24,25,26,27].

In the computer program, the linear and the quadratic forms of artificial viscosity are provided[24]. Both are related to the rate of compression of the material. When the material is expanding the artificial viscosity is zero. The linear form of the artificial viscosity can be expressed as[24]:

$$Q = C_1 C_s A \frac{\Delta\rho}{\Delta t} \qquad (3.5)$$

where C_1 is the coefficient of linear artificial viscosity

C_s is the speed of sound in the material

A is the area of the cell (X-Y plane) and

$\Delta\rho$ is the change in density over the time step it.

The quadratic form can be expressed as[24]

$$Q_q = \frac{C_q A}{\rho} \left(\frac{\Delta\rho}{\Delta t}\right) \qquad (3.6)$$

where C_q is the coefficient of quadratic artificial viscosity.

The artificial stress Q is:

$$Q = Q_1 + Q_q$$

where Q_1 is the stress due to the linear artificial viscosity and Q_q is the stress due to the quadratic artificial viscosity.

3.7 *Calculation of Sound Speed*

The sound speed is calculated for every cell at each cycle. It is given by the following relationship[25]:

$$C^2 = \left(\frac{\partial P}{\partial \rho}\right)_S = -V^2 \left(\frac{\partial P}{\partial V}\right)_S \quad \text{or}$$

$$C^2 = -V^2 \left[\left(\frac{\partial \rho}{\partial E}\right)_V \left(\frac{\partial P}{\partial V}\right)_S + \left(\frac{\partial P}{\partial V}\right)_E \left(\frac{\partial V}{\partial V}\right)_S \right] \text{ or}$$

$$C^2 = V^2 \left[P \left(\frac{\partial P}{\partial E}\right)_V - \left(\frac{\partial P}{\partial V}\right)_E\right] \qquad (3.8)$$

The derivatives are obtained by using the Gruneisen equation of state and the shock jump conditions.

The time step is controlled so that the stability requirements are met. The time step is taken to be a fraction (less than 0.9) of the ratio $\Delta x/C$ where Δx is the minimum cell dimension and C is the local sound speed.

3.8 *Results*

In order to evaluate the predictions of the code its results were compared to available experimental results. As a test the relationship between plexiglas pressure and plexiglas thickness for the standard donor of the gap test was used.

Figure 32 illustrates both the experimental and the calculated curves. The agreement is good and therefore the results of the code reliable. Figure 33 shows pressure histories for various points along the axis of symmetry of the experiment. Table 5 shows the HOM equation of state parimeters for the donor charge and Table 6 shows the HOM parameters for the plexiglas attenuator[10].

After testing the code the gap tests were modelled.

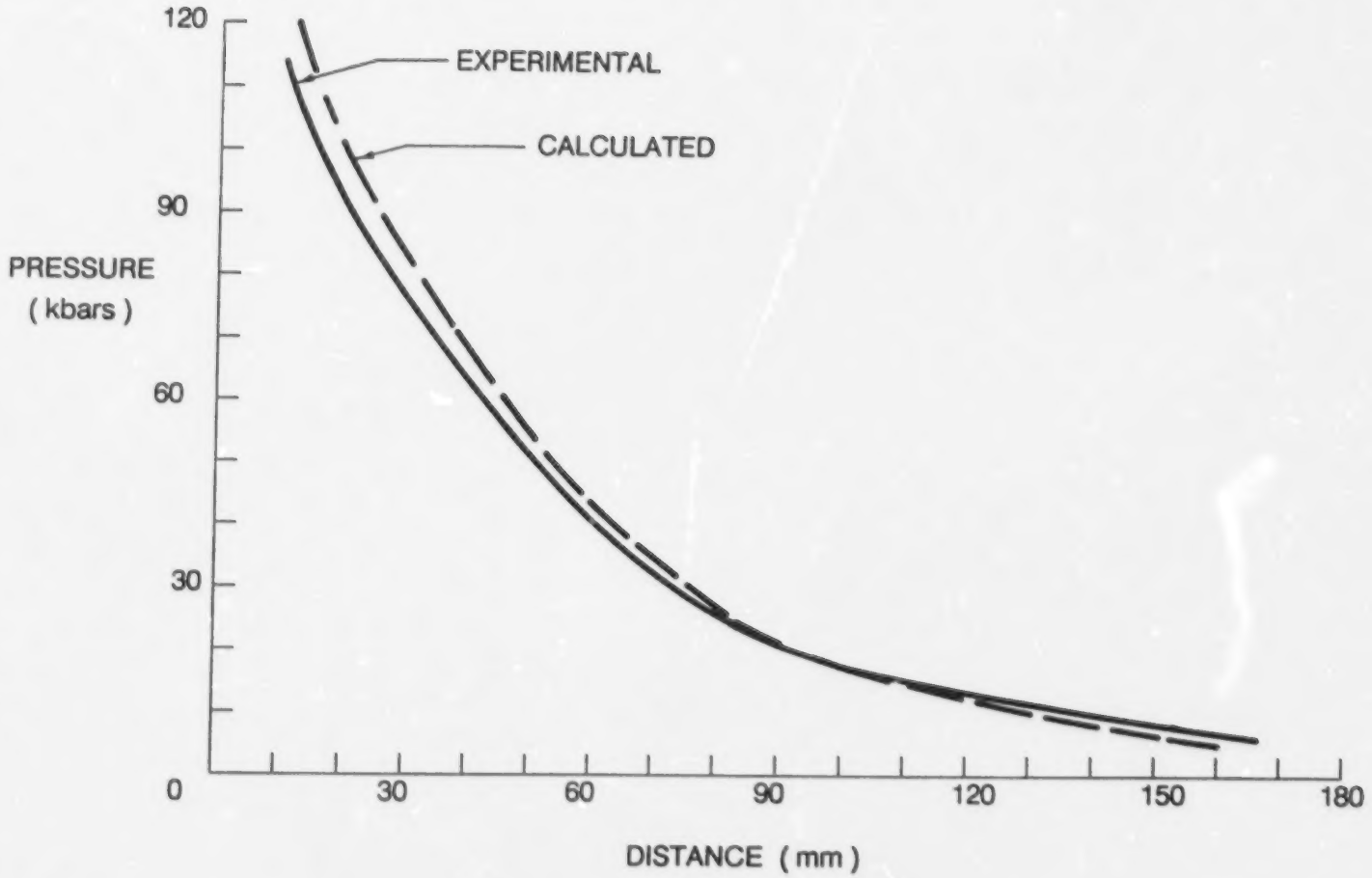

FIGURE 32: EXPERIMENTAL AND CALCULATED CURVES SHOWING PLEXIGLAS PRESSURE AS A FUNCTION OF DISTANCE IN THE CALIBRATED GAP TEST.

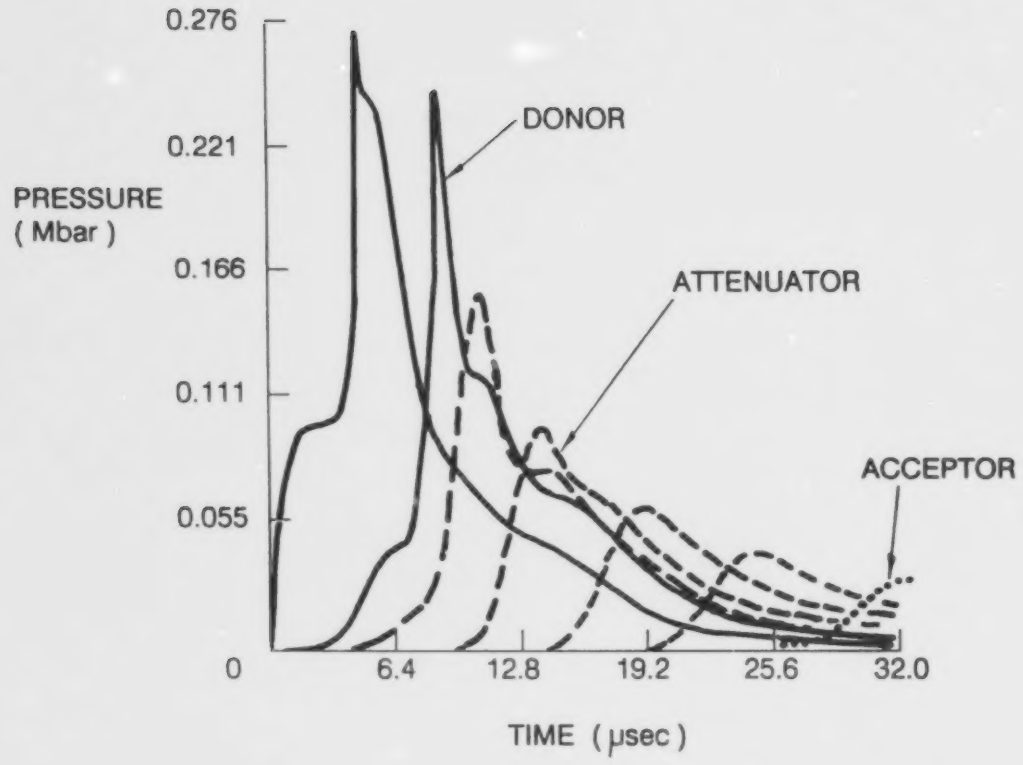

FIGURE 33: TYPICAL PRESSURE HISTORIES FOR VARIOUS POINTS ALONG THE AXIS OF THE GAP TEST ARRANGEMENT.

TABLE 5: HOM EQUATION OF STATE PARAMETERS FOR THE DONOR CHARGE

UNREACTED EXPLOSIVE	DETONATION PRODUCTS
C = 1.328000000 E-01	A = -3.493161198 E 00
S = 1.993000000 E 00	B = -2.515816593 E 00
F = 1.148792449 E+01	C = 3.069129255 E-01
G = 2.942381533 E+01	D = -1.262333797 E-02
H = 5.140788160 E+01	E = -6.177628658 E-03
I = 3.666680381 E+01	K = -1.544599843 E 00
J = 1.077530936 E+01	L = 5.018500217 E-01
γ = 1.730000000 E 00	M = 7.050235632 E-02
C_V= 2.930000000 E-01	N = 5.088893103 E-03
V_0= 6.250000000 E-01	O = 1.4841118028 E-04
α = 0.000000000 E 00	Q = 7.473112216 E 00
	R = -4.683137299 E-01
	S = 4.079025664 E-02
	T = 4.985623550 E-02
	U = -1.759735317 E-02
	C_V= 5.650000000 E-01
	Z = 1.000000000 E-01

TABLE 6: HOM EQUATION OF STATE PARAMETERS FOR THE PLEXIGLAS ATTENUATOR[10]

C =	2.43800000000 E-01
S =	1.57850000000 E-00
F =	5.29380243506 E 00
G =	-4.24950371368 E 00
H =	-1.55055576332 E 01
I =	-3.08638075572 E 01
J =	-1.46708193739 E 01
γ =	2.15700000000 E 00
C_V =	0.00000000000 E 00
V_0 =	8.47457627000 E-01
α =	0.00000000000 E 00

According to the experiments the critical gap thickness for pressed RDX was 120mm. The calculation yielded a value of 1476KJ/m^2 for the critical energy required to ignite the charge.

The critical energy is calculated as

$$E_{cr} = \int_0^t P\, U_p \, dt$$

where P is the pressure

U_p is the particle velocity

t is the duration of interest. This is the time until the paricle velocity vector has a direction opposite to the direction of the propagation of the initial shock wave created by the impact.

It should be noted that HOM parameters are required for the acceptor charge. The acceptor charge is assumed to be unreacted since only the energy given to it by the shock wave is of interest. Since no reactive model is assumed for the acceptor only parameters for the solid product are required.

In the case of waxed and pressed RDX the same parameters used for the donor were used.

According to the experiments, the critical thickness of the attenuator for ignition of the emulsion was 110mm. This was modelled in order to calculate the critical energy for ignition. This was found to be 2430KJ/m^2 . Table 7 shows the HOM equation of state parimeters for the unreacted slurry which were used in the modelling.

The experimental critical gap thickness for the slurry was found to be 140mm. The calculated critical energy was found to be equal to 672KJ/m^2 . The HOM equation parameters for the slurry are shown in Table 8.

The cell dimensions for the various materials was 0.50cm x

TABLE 7: HOM EQUATION OF STATE PARAMETERS FOR THE UNREACTED SLURRY

C = 1.30000000000 E-01

S = 1.60000000000 E-00

F = 5.46000000000 E 00

G = -2.10820000000 E 00

H = -3.81070000000 E 00

I = -4.36040000000 E 00

J = 2.42500000000 E 00

γ = 1.50000000000 E 00

C_V = 5.00000000000 E 01

V_0 = 0.87000000000 E-00

α = 0.00000000000 E 00

TABLE 8: HOM EQUATION OF STATE PARAMETERS FOR THE UNREACTED EMULSION

C = 1.30000000000 E-01

S = 1.60000000000 E 00

F = 5.46000000000 E 00

G = -2.10820000000 E 00

H = -3.81070000000 E 00

I = -4.36040000000 E 00

J = 2.42500000000 E 00

γ = 1.50000000000 E 00

C_V = 5.00000000000 E-01

V_0 = 0.87000000000 E-00

α = 0.00000000000 E 00

0.50cm throughout the calculations. Furthermore it was assumed that the system was donor-acceptor was confined by a cylindrical shell of plexiglas. The shell thickness was 2.0cm.

3.9 *Discussion*

It is obvious that the slurry exhibited considerably lower critical energy for ignition due to low amplitude shocks. Therefore it is expected that the slurry will be more susceptible to accidental initiation than the other two products. The projectile data showed the same trend as far as the emulsion and the slurry are concerned. The emulsions were harder to detonate. According to the findings of the modified gap test they are more difficult to ignite.

The emulsion was somewhat more sensitive than the RDX. This is due to the high density of the waxed RDX. One would expect RDX to be more sensitive than the emulsion at the same density (ρ=1.18 g/cc).

Kroh et al[12] have obtained critical energies for a variety of military explosives. Their values are shown in Table 9 . It follows that the explosives tested are considerably more sensitive than the ones of Table 9. Dobratz[29] however has reported critical energies of 1500KJ/m and 600KJ/m for Composition B and PBX 9404 respectively. It follows that the explosives tested are in this range of sensitivity with waxed RDX being closer to Composition B and Slurry type A closer to PBX 9404.

For comparison purposes it is interesting to calculate and discuss the critical energies required for a positive event produced by impact in experiments other than the modified gap test.

TABLE 9: CRITICAL ENERGIES FOR VARIOUS EXPLOSIVE COMPOSITIONS[22,29]

EXPLOSIVE	DENSITY (g/cc)	CRITICAL ENERGY FOR IGNITION (KJ/m^2)
HNS	1.60	3600
HMX/PB (85/15)	1.71	2500
RDX/Al/Pb (67/18/15)	1.65	3400
RDX/Al/Pb (71/14/15)	1.65	2400
Compostion B	1.72	1500
PBX 9404	1.82	630

In projectile impact the positive event normally refers to the detonation of the impacted explosive. According to the available projectile data the slurry detonated when impacted by an aluminum projectile having diameter of 2.5 cm and length of 5.0 cm travelling at a velocity of 447 m/s. Modelling of the experiment and assuming no reaction of the slurry, the energy due to the impact was calculated to be 1202 KJ/m^2.

For the detonation of the emulsion in projectile impact experiments, a brass projectile having diameter and length of 13 mm and trevelling at a velocity of 850 m/s was required. The calculated energy for this case was 4142 KJ/m^2.

According to data presented by Persson[31] RDX/oildetonated when impacted by a brass projectile having diameter and length of 15 mm. The density of the composition was 1.50 g/cc, which is slightly higher than the density of the RDX in the experiments of this work (ρ=1.55g/cc). The calculated energy for this case was 2078 KJ/m^2.

Watson and Hay[16] have reported that air bubble sensitizes Nitromethane is very sensitive to impact. According to their data[16] ignition of the Nitromethane would take place after impact by a steel projectile (diameter 10.0 cm and length 13.3 cm) moving at a velocity of 25 m/s. The impacted explosive was completely contained. Therefore it can be assumed that the kinetic energy of the projectile would all be degraded to heat after impact. Therefore the critical impact energy is

$$E_k = \frac{1}{2} m u^2 = \frac{1}{2} 8.083\ 25^2 = 25.26 \text{ KJ}$$

This expressed as energy per unit area is

$$E = \frac{25.26}{\text{area}} = \frac{25.26}{(0.05^2\ \pi)} = 321.6 \text{ KJ/m}^2.$$

The calculated energy, assuming rigid boundaries was 316

KJ/m^2.

Energy values have also been reported for drop weight impact tests. However these tests use a very small quantity of explosive which is not necessarily representative of the bulk of the explosive (density discontinuities, chemical composition etc.) and the response of the sample is not characterized clearly. Usually the response is reported as an explosion, however the term "explosion" covers everything from a mild deflagration to a detonation. Furthermore the size of the sample is below the critical diameter of most explosives and the density of the sample can be very different than the original density of the explosive. A change in the density definitely changes the sensitivity.

Another drawback of the impact tools is that they are not standardized. Lawrence Livermore Laboratory uses a weight of 2.5-5 Kg which is dropped from a pre-set height onto a small sample of explosive (approximately 35 mg)[29]. The Swedish Detonic Foundation uses a modified Kast apparatus[31]. USBM has used a large impact tester in which an 80g sample is impacted by a 200 Kg weight[31]. The drop test mostly used today consists of a 5 Kg free falling weight. The maximum height is 330 mm and sometimes a sandpaper is placed under the sample. Many military and a few commercial explosives have been tested by this apparatus. According to Chan[32] typical critical energy levels for a slurry, emulsion and RDX are 40-150 KJ/m^2, 150-350 KJ/m^2 and 40-70 KJ/m^2 respectively. However the determination of an "explosion or reaction" is based on visual or aural observations. Any indication of decomposition (explosion, burning, flash, smoke or charring) is considered a "go". Therefore the levels of energy mentioned before cannot differentiate between ignition,

deflagration or detonation. Furthermore the mechanism responsible for the decomposition of the tested explosive is not exactly known. Initially the explosive is subjected to a shock pressure, then to the reverberations of the shock wave and then it flows radially at a high speed. This radial flow can create viscous heating which can cause decomposition. Moreover if a sand paper is used frictional heating can contribute to the process.

It is obvious that the critical energy levels are different for each type of experiment.

The drop weight impact experiment requires the least amount of energy. However the mechanism responsible for the start of decomposition is complicated and significantly different than the mechanisms of the other experiments.

Watson's experiment on the bubble sensitized Nitromethene required relatively small amounts of energy to result in an explosion. The result though is not well defined and the term "explosion" is used as a general term indicating a violent reaction.

The modified gap tests determined energy levels for the start of sufficient amount of decomposition to change the pressure - particle velocity relationship which is obtained for an unreacted explosive. The reaction is caused by the single passage of a low amplitude shock wave and does not necessarily result in a detonation.

Finally the projectile tests required significant amounts of energy to shock initiate the explosive.

It appears that each experiment requires energy the amount of which depends on the degree of reaction (deflagration, detonation) and the mechanism leading to decomposition (shock,

friction, viscous flow). Each test examines the behaviour of the explosive under different conditions. The modified gap tests together with hydrodynamic modelling find the critical energy required for the ignition of an explosive subjected to a single impact by a low amplitude shock wave.

4.0 *CONCLUSION*

A method for characterizing commercial explosives with regard to their low velocity impact sensitivity has been selected and applied in the case of a slurry and an emulsion explosive.

Waxed and pressed RDX was examined as well for comparison.

The method, which consists of calibrated gap tests and hydrodynamic modelling of the tests to calculate critical energies, yielded low amplitude shock sensitivity for all three explosives.

Two thresholds, one for burning and one for detonation could be identified by interpreting the experimental pressure particle velocity curves. The air bubble sensitized slurry was found to be more sensitive than the microballoon sensitized emulsion and the waxed and pressed RDX (ρ=1.55g/cc).

Critical energies for burning were calculated for modelling a gap test with attenuator thickness equal to that which would result in a shock pressure equal to the critical shock pressure determined by the pressure-particle velocity curve of the explosive. The critical energies quantify the low amplitude shock sensitivity of the explosive since they describe the critical conditions for the start of burning (ignition) due to the passage of a shock wave.

Modelling of the projectile impact tests yielded much higher critical energies. This is due to the fact that the modelling examined critical conditions for the shock initiation of the explosives.

The drop weight tests have yielded lower values for the

critical energies. This is due to the mechanism responsible for the ignition or initiation of the charge which is different than that of the gap tests (single shock).

Similarly, the Susan test investigates the shock sensitivity of explosives due to impact crushing and pinch. Therefore the critical energies obtained by this test are representative of the conditions it investigates.

Different mechanisms are responsible for the ignition and initiation of explosives tested by the various tests. Therefore the theoretical investigation of each test is necessary in order to calculate the critical conditions imposed by the various mechanisms.

ACKNOWLEDGEMENTS

I would like to express my sincere thanks to the following:

-John Moroz and Guillermo Silva for their help in performing the calibrated gap tests.

-Raymond D. Heater for the performance of the projectile tests.

REFERENCES

1. Walker, F.G. and Wasley, R.J.: "Critical Energy for Shock Initiation of Heterogeneous Explosives", Explosivstoffe 17,No. 9, 1969.

2. Sixth International Symposium on Detonation: "Discussion on Shock Initiation and P^2t", Office of Naval Researach, Department of the Navy, Arlington, Virginia, 1976.

3. Hayes, D.B. "A Detonation Criterion from Thermal Explosion Theory", 6th International Symposium on Detonation, 1976.

4. Moulard, H.: "Critical Area Concept for the Initiation of Solid High Explosives by the Impact of Small Projectiles" Progress in Astronautics and Aeronautics, Vol. 75, 1979 pp. 296-302.

5. Lee, E.L., Tarver, C.M.: "Phenomenological Model of Shock Initiation in Heterogeneous Explosives", Phyics of Fluids, Vol. 23, No. 12, pp. 2362-2372, Dec. 1980.

6. Green, L.G., James, E., Lee, E., Chambers, E., Tarver, C., and Westmoreland, C.: "Delayed Detonation in Propellants from Low Velocity Impact", 7th International Symposium on Detonation, 1981, pp. 256-264.

7. P. Katsabanis: "Numerical Modelling of Explosives Performance

and Sensitivity" Ph.D. Thesis, Queens University, Kingston, 1987.

8. Forest, C.: "Burning to Detonation", Los Alamos Scientific Laboratory, LA-7245, 1978.

9. Forest, C.: "Burning and Detonation", 7th International Symposium on Detonation, 1981, pp. 234-242.

10. Mader, C: "Numerical Modelling of Detonations" University of California Press, 1979.

11. Forest, C and Mader C.: "Numerical Modelling of the Deflagration to Detonation Transition", 17th International Symposium on Combustion, 1976, pp. 35-41.

12. Bruckman, H.J. and Guillet, J.E.: "Theoretical Calculations of Hot-spot Initiation in Explosives", Canadian Journal of Chemistry, Vol. 46, 1968, pp. 3221-3228.

13. Napadensky, H.: "Initiation fo Explosives by Low Velocity Impact", 4th International Symposium on Detonation", 1965, pp. 473-476.

14. Smith, L.C. and Craig, B.G.: "Primer on SDT, DDT, XDT, Pick-up and Sympathetic Detonation 16th JANNAF Combustion. Meeting, Naval Postgraduate School, Monterey, California, 1979.

15. Green, L.G. and Dorough, G.D.: "Further Studies on the Ignition of Explosives" 4th International Symposium on Detonation", 1965, pp. 477-486.

16. Hay, J.E. and Watson, R.W.: "Initiation of Detonation in Insensitive Liquid Explosives by Low Amplitude Compression Waves", 6th International Symposium on Detonation, 1976, pp. 115-123.

17. Frey, R., Melani, G., Chawla, M. and Trimble, J.: "Initiation of Violent Reaction by Projectile Impact" 6th International Symposium on Detonation, 1976, po. 325-335.

18. Bowman, A.L., Forest, C.A., Kershner, J.D., Mader, C.L., Pimbley, G.H.: "Numerical Modelling of Shock Sensitivity Experiments" 7th International Symposium on Detonation, Naval Surface Weapons Center, 1981.

19. Jensen, R., Bloomer, E. and Brown, B.: "An Instrumented Shotgun Facility to Study Impact Initiated Explosive Reactions", 7th International Symposium on Detonation, 1981, pp. 299-307.

20. Tasker, D.G.: "Shock Initiation and Subsequent Growth of Reaction in Explosives and Propellants: The Low Shock Initiation Test, LASI". , 7th International Symposium on Detonation, 1981.

21. Liddiard, T.P. and Forbes, J: "Initiation of Burning and

Detonation in Cast H-6 and Cast PBXW-109" ,7th International Symposium on Detonation, 1981, pp. 308-315.

22. Kroh, M, Thoma, K., Arnold, W. and Wollenweber, V.: "Shock Sensitivity and Performance of Several High Explosives", 8th International Symposium on Detonation, 1985, pp. 502-508.

23. P. Katsabanis: "Experimental Evaluation of a High Velocity Impact Model for Commercial Explosives" Final Report, CANMET, Proj. Number : 110702, 1985.

24. Seaman, L.: "TROTT Computer Program", Stanford Research Institute, 1976.

25. Shaw, M.S. and Straub, G.K.: "HYDROX : A One Dimensional Lagrangian Hydrodynamics Code" Los Alamos Scientific Laboratory, LA-8642-M, March 1981.

26. Cowperthwaite, M. and Zwisler, W.H.: "Theoretical and Mathematical Formulations for the Tiger Computer Program" Stanford Research Institute, California, 1973.

27. Zukas, J., Nicholas, T., Swift, H., Greszczuk, L., Curran, D.: "Impact Dynamics", John Wiley & Sons, 1982.

28. Potter, D.: "Computational Physics", Prentice Hall Press, London, 1972.

29. Dobratz, B.M.: "Properties of Chemical Explosives and

Explosives Simulants" LLNL Explosives Handbook, March 16, 1981.

30. Marsh, S.P.: "LASL Shock Hugoniot Data" University of California Press, 1980.

31. Johansson, C.H. and Persson, P.A.: "Detonics of High Explosives", Swedish Detonic Research Foundation, Academic Press, 1970.

32. Feng, K.K.: Private communication.

33. Mader, C.L.: "Numerical Modelling of Detonation", Videotaped Lectures, Los Alamos Scientific Laboratory, 1979-1983.